Trace element constraints on mantle sources during mid-Proterozoic magmatism: evidence for a link between the Gardar (South Greenland) and Abitibi (Canadian Shield) mafic rocks

Ralf Halama, Jean-Louis Joron, Benoît Villemant, Gregor Markl, and Michel Treuil

Abstract: Trace and major element compositions of mid-Proterozoic (1.20–1.16 Ga) basaltic lava flows and dikes from the Gardar Province (South Greenland) provide evidence for two geochemically distinct magma sources. Based on distinct features of incompatible trace element ratios, such as Th/Ta, Th/Tb, or Th/Hf, they differ by the composition of their mantle source and by their partial melting trends. One mantle source is compositionally transitional between mid-ocean ridge basalt (MORB)-type and ocean-island basalt (OIB)-type sources with relatively low Ta/Hf ratios (~0.2), moderate enrichment in light rare-earth elements (LREE), and slightly positive initial ε_{Nd} values (+2). It can be attributed to either a lithospheric mantle source or a depleted astenospheric mantle plume component that has been enriched shortly prior to eruption. The other mantle source is characterized by high Ta/Hf ratios (~0.6), a more pronounced LREE enrichment, and initial ε_{Nd} values around 0. Elevated Ce_N/Yb_N (7.0–9.8) and Tb_N/Yb_N ratios (1.6–1.8) of the rocks derived from this source indicate the presence of garnet during melting, suggesting melt generation at depths > 70 km. This mantle source has the geochemical characteristics of an OIB-type source and is interpreted as originating from a mantle plume. Samples from the slightly younger (1.14 Ga) Abitibi dike swarm (Superior Province, Canada), spatially connected to the Gardar Province, show very similar trace element characteristics and the same two distinct magma sources can be identified. The geochemical similarities between the magma sources in South Greenland and Canada support the idea of a genetic link between the two magmatic provinces. This link strengthens the idea that the system was a long-lived major intracontinental rift zone.

Résumé : Les compositions des éléments majeurs et des éléments traces dans des coulées de lave et des dykes basaltiques datant du Protérozoïque moyen (1,20–1,16 Ga), provenant de la province de Gardar (sud du Groenland), fournissent des évidences de deux sources de magma géochimiquement distinctes. Selon les caractéristiques distinctes de rapports incompatibles d'éléments traces, tels que Th/Ta, Th/Tb ou Th/Hf, la source mantellique et les fusions partielles de ces coulées de lave seraient différentes. Une des sources mantelliques a une composition de transition entre les sources de type basalte de la dorsale médio-océanique (MORB) et de type basalte océanique insulaire (OIB) avec des rapports Ta/Hf relativement faibles (~0,2), un enrichissement modéré en éléments des terres rares légers et des valeurs ε_{Nd} initiales légèrement positives (+2). Ce magma peut être attribué à une source mantellique lithosphérique ou à une composante d'un panache appauvri du manteau asthénosphérique qui a été enrichi peu de temps avant l'éruption. L'autre source mantellique est caractérisée par des rapports Ta/Hf élevés (~0,6) et un enrichissement plus prononcé en éléments des terres rares légers et des valeurs ε_{Nd} initiales autour de 0. Les rapports élevés Ce_N/Yb_N (7,0–9.8) et Tb_N/Yb_N (1,6–1,8) de roches provenant de cette source indiquent la présence de grenat durant la fusion, suggérant ainsi une génération de produits fondus à des profondeurs supérieures à 70 km. Cette source mantellique a les caractéristiques géochimiques d'une source de type OIB et elle est interprétée comme provenant d'un panache du manteau. Des échantillons de l'essaim de dykes, légèrement plus jeune (1,14 Ga), de l'Abitibi (province du Supérieur, Canada), relié dans l'espace à la province de Gardar, montrent des caractéristiques d'éléments traces très similaires et les mêmes deux sources de magma. Les ressemblances géochimiques entre les sources de magma dans le sud du Groenland et le Canada soutiennent l'idée d'un lien génétique entre les deux provinces magmatiques. Ce lien supporte l'idée que le système a été une zone de distension intracontinentale majeure de longue durée.

[Traduit par la Rédaction]

Received 9 March 2006. Accepted 20 September 2006. Published on the NRC Research Press Web site at http://cjes.nrc.ca on 18 May 2007.

Paper handled by Associate Editor J. Greenough.

R. Halama[1,2] and B. Villemant. Equipe Volcanologie, IPGP-CNRS, case courrier 89, 4 Place Jussieu, 75005 Paris, France.
J.-L. Joron and M. Treuil. Groupe des Sciences de la Terre, Laboratoire Pierre Süe – CE Saclay, 91191 Gif sur Yvette cedex, France.
G. Markl. Institut für Geowissenschaften, Universität Tübingen, Wilhelmstr. 56, 72074 Tübingen, Germany.

[1] Corresponding author (e-mail: rh@min.uni-kiel.de).
[2] Present address: Institut für Geowissenschaften, Christian-Albrechts-Universität Kiel, 24098 Kiel, Germany.

Can. J. Earth Sci. **44**: 459–478 (2007) doi:10.1139/E06-108

Introduction

The study of mantle source components of basaltic rocks in the geological record is essential for an improvement in our understanding of mantle dynamics and the geochemical evolution of the Earth's mantle. Trace element and isotope geochemistry can be used to assess the involvement of known mantle reservoirs, if their characteristics are not overprinted by crustal contamination (Weaver 1991; Hart et al. 1992). Two or more distinct mantle sources were identified for mafic dike swarms (Condie et al. 1987; Tarney and Weaver 1987; Cadman et al. 1993), intraplate volcanic fields (Cook et al. 2005), and rift-related magmatism (Barrat et al. 1990), even intercalated within a single lava pile (Wilband and Wasuwanich 1980). Mantle sources of intracontinental magmatism are usually compared with mantle components identified in oceanic settings and are often interpreted as mixtures between them (Franz et al. 1999; Cebriá et al. 2000; Cook et al. 2005). The commonly invoked end-member mantle reservoirs are depleted mid-ocean ridge basalt (MORB) mantle (DMM; that is, the upper mantle source for mid-ocean ridge basalts), several types of enriched components (enriched mantle (EM)1, EM2, high-U/Pb mantle (HIMU)) identified in ocean-island basalt (OIB), and the focus zone (FOZO), which is based on a region of convergence of arrays in Pb, Sr, and Nd isotope space (Hart et al. 1992). The enriched components may be derived from recycling of ancient oceanic crust and lithosphere associated with pelagic or terrigenous sediments (Hofmann and White 1982; Chauvel et al. 1992; Eisele et al. 2002). Alternative explanations include recycling of subcontinental lithosphere (Hawkesworth et al. 1986) and metasomatic enrichment of the oceanic lithosphere (Sun and McDonough 1989; Pilet et al. 2005), although a lower mantle origin for both HIMU and EM1 has also been proposed (Bell and Tilton 2001). FOZO may represent material from the lower mantle that is present as a mixing component in deep mantle plumes (Hart et al. 1992).

The role of mantle plumes, active at least since 3500 Ma (Ernst and Buchan 2001), is of particular interest because they are considered to play an important role in continental breakup, uplift, and lithospheric thinning (Davies 1999; Condie 2001). Mantle plumes are also thought to be involved in the generation of large igneous provinces, giant dike swarms, carbonatites, and kimberlites (Morgan 1971; Coffin and Eldholm 1994; Ernst and Buchan 1997; Bell and Tilton 2001). Rifting is often preceded by plume-related activity (Courtillot et al. 1999) and pre-existing rifting can help localize plumes (Ernst and Buchan 2002). However, many features commonly associated with plumes may alternatively be related to high-fertility patches in the mantle or tectonically or stress-controlled features (Anderson 2005; McHone et al. 2005). Thus, the concept of mantle plumes introducing chemical heterogeneities into the upper mantle is still debated (Anderson 2000; Foulger et al. 2005), and mantle models where chemical heterogeneities are caused by remixing of the entire subducted crust into the convecting mantle without the presence of plumes have also been proposed (Fitton and James 1986; Smith 2005). Whatever the ultimate origin of chemical heterogeneities in mantle-derived magmas, their chemical signatures are useful tracers of mantle-source compositions (Schilling 1973; Hofmann 2003).

The Gardar Province of South Greenland is a rift-related igneous province with magmatic activity lasting from about 1.35 to 1.14 Ga (Upton and Emeleus 1987; Upton et al. 2003). During late-Gardar (1.20–1.14 Ga) activity, basaltic lavas of the Eriksfjord Formation and two major dike swarms were emplaced in the Gardar Province. The available geochemical data have been interpreted as evidence for either an OIB-type mantle source (Coulson et al. 2003; Halama et al. 2003) or a lithospheric source (Goodenough et al. 2002). The Gardar magmatic activity is classified as "probably linked to a mantle plume" in the compilation of Ernst and Buchan (2001). It has been linked to the contemporaneous activity on the Canadian Shield (Ernst and Buchan 2002), forming a large tectonomagmatic Proterozoic structure that is comparable in size to the present day East African Rift (Macdonald and Upton 1993). In particular, the 1.14 Ga old Abitibi dike swarm (Superior Province, Canada) is thought to be spatially connected to the late-Gardar dikes (Fig. 1), and a link to the Keweenawan Rift has also been proposed. Moreover, the Abitibi dikes have been linked to an OIB-type mantle source and a mantle plume (Ernst and Bell 1992; Ernst and Buchan 2001). In this study, we present new trace element data of basaltic rocks of late Gardar and Abitibi activity, focusing on highly incompatible trace elements such as Th, Ta, Hf, and Tb; these elements are relatively immobile during metamorphism and alteration processes, and can be used to trace mantle heterogeneities (Joron and Treuil 1989; George and Rogers 2002). It is the aim of this study to investigate geochemical similarities of the Gardar and Abitibi mantle sources, to evaluate possible mantle plume contributions, and to model the conditions of partial melting.

Geological setting

The Gardar Province in South Greenland is an example where mid-Proterozoic rift-related magmatic activity (1.35–1.14 Ga) produced a wide variety of rocks including basalts, syenites, and carbonatites (Upton et al. 2003). Samples analyzed in this study include basalts from the volcano-sedimentary Eriksfjord Formation (EF) and gabbroic dike rocks (diabase) from the Nunarssuit–Isortoq dike swarm (Fig. 1). The EF represents a ~3500 m thick sequence of supracrustal rocks comprising continental sandstones and conglomerates, and lava flows and sills of basaltic to phonolitic composition (Larsen 1977). It is subdivided stratigraphically into lower, middle, and upper lavas. The rocks lie unconformably on calc-alkaline granitoids of the 1.85–1.79 Ga old Julianehåb batholith (Garde et al. 2002) and are cut by the 1160 ± 5 Ma old Ilímaussaq intrusion (Krumrei et al. 2006). Two Sm–Nd isochron ages of the middle lavas gave 1.17 ± 0.03 and 1.20 ± 0.03 Ga (Paslick et al. 1993). High eruption rates are inferred for the volcanic system, based on paleomagnetic data and the lack of erosion and palaeosol development between flows (Piper et al. 1999).

The Nunarssuit–Isortoq dike swarm (1190 ± 44 Ma) comprises a variety of alkaline rocks ranging from gabbros to syenites. Together with the Tugtutôq–Ilímaussaq swarm, which includes the 1163 ± 2 Ma old Giant dike complexes of Tugtutôq (Buchan et al. 2001), it represents one of the two major dike swarms emplaced into the Julianehåb batholith along WSW–ENE to southwest–northeast faults in the late-

Fig. 1. (*a*) Schematic sketch map of the reassembled Laurentia, showing the collinearity of the Gardar and Abitibi dikes (modified after Macdonald and Upton 1993). (*b*) Simplified map of the northeast-trending Abitibi dikes in the southern Superior Province (after Ernst and Buchan 1993) with sample locations as given in Macouin et al. (2003). (*c*) Simplified map of the Gardar Province (modified after Upton and Emeleus 1987) with sample locations (for details, see Halama et al. 2003, 2004).

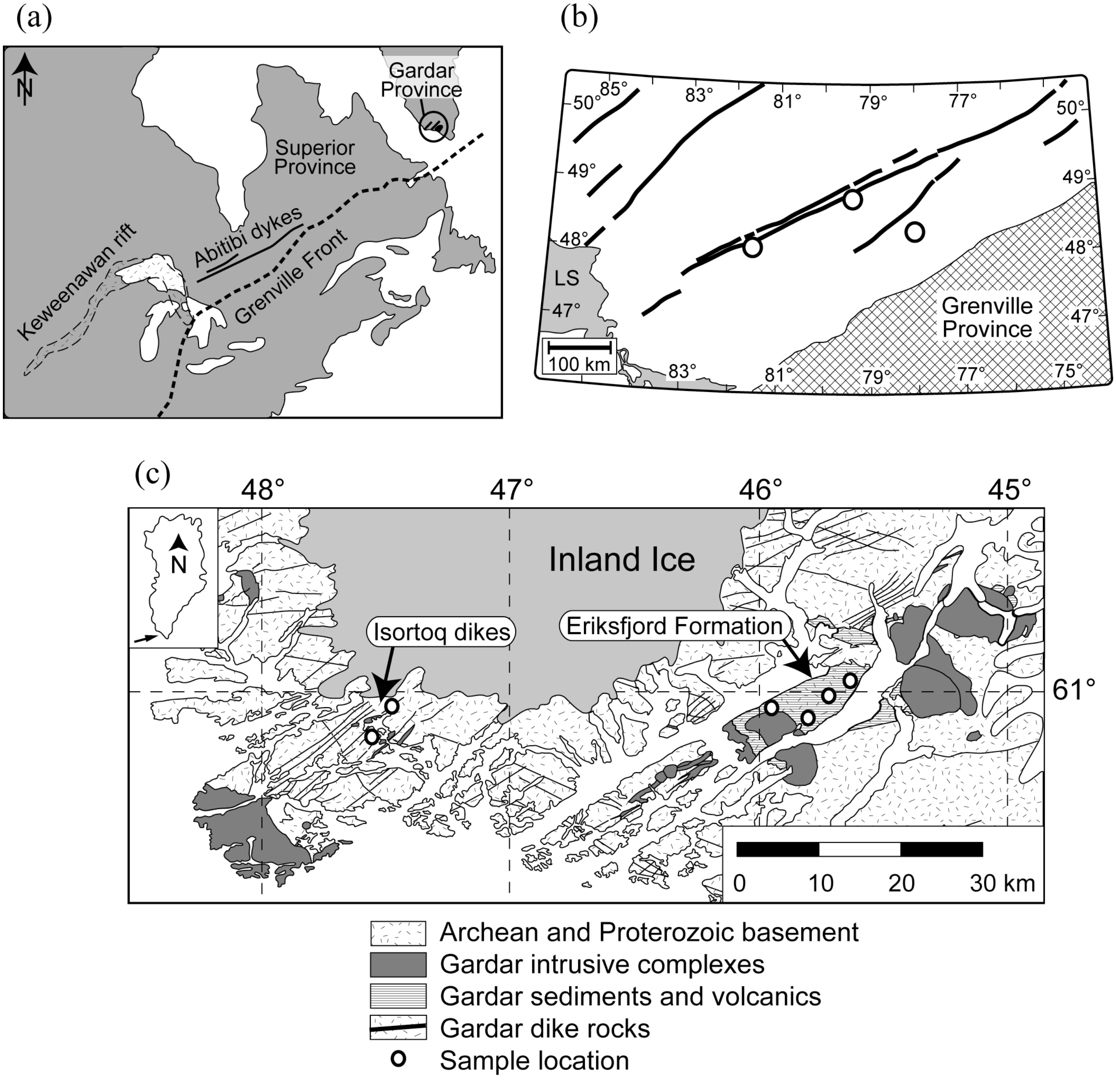

Gardar period. Although the dikes were emplaced into upper crustal rocks, the most likely crustal contaminant of the basaltic magmas is thought to be lower crustal material, similar in composition to the granitic gneisses of the Northern Border Zone (NBZ), which is located south of the Archean craton (Halama et al. 2004).

The Abitibi dike swarm (Fig. 1) intruded the Superior Province, an Archean block amalgamated during the Paleoproterozoic to form Laurentia (Hoffman 1989). It comprises a number of widely spaced, nearly vertical dikes that trend northeast and vary in thickness from 15 to 250 m (Ernst and Buchan 1993; Buchan and Ernst 2004). The 1140.6 ± 2 Ma old Great Abitibi dike (Krogh et al. 1987) is the most prominent member of the Abitibi swarm and can be traced for at least 700 km (Ernst and Bell 1992). The Abitibi dikes mark a failed rift arm associated with Keweenawan rifting, and they are assumed to be related to the same magmatic event because of their geochemical similarities (Condie et al. 1987; Fahrig 1987). They fan slightly away from the rift (Ernst and Buchan 1993), possibly because extensional stress orientations vary across large distances in the lithosphere (McHone et al. 2005). The Abitibi rocks vary from olivine-

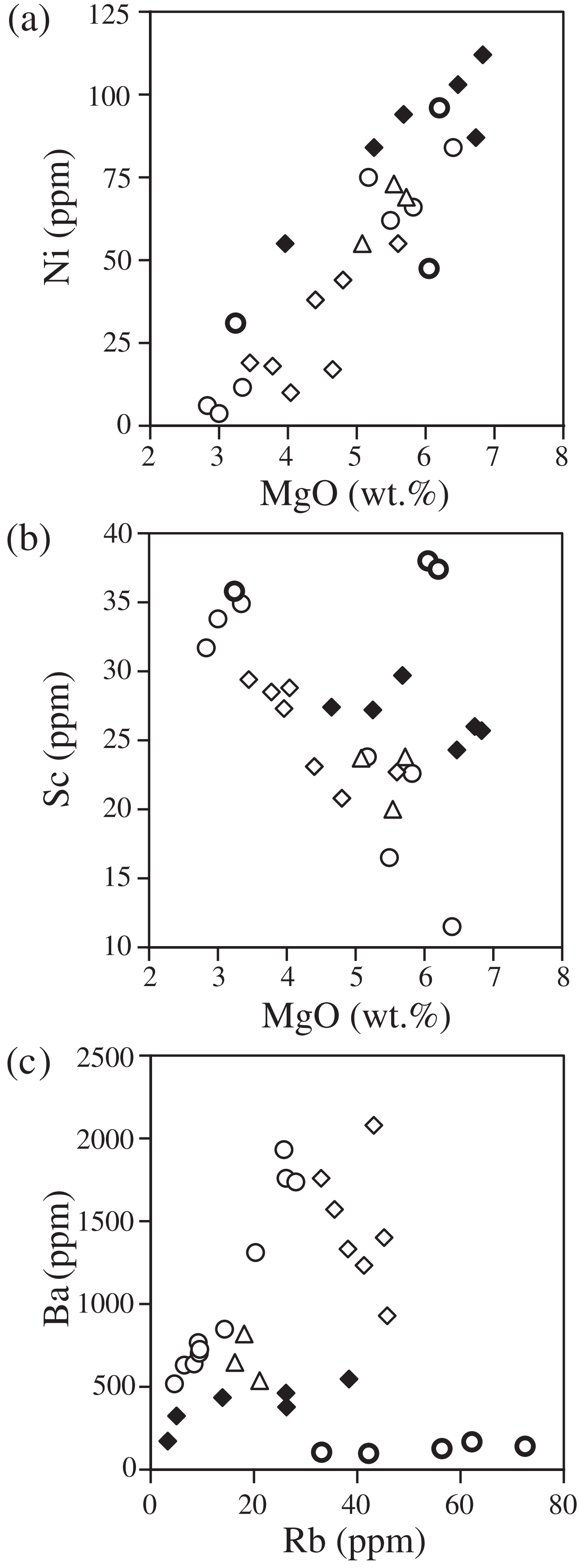

Fig. 2. Fractionation and element mobility in Gardar and Abitibi samples. (*a*) Positive correlation between Ni and MgO, indicative of olivine fractionation. (*b*) Lack of a positive correlation between Sc and Mg, suggesting absence of significant clinopyroxene fractionation. (*c*) Ba vs. Rb plot, showing good correlations for the Abitibi samples, but broad scatter for the Gardar samples, interpreted to reflect Rb mobility. ◆, Eriksfjord Formation (EF) basalts, lower and middle lavas; ◇, EF basalts, upper lavas; △, Isortoq dikes; **O**, Abitibi dikes, Group 1a; ○, Abitibi dikes, Group 2.

gabbros to monzodiorites and show an alkaline affinity (Ernst and Bell 1992). The late-Gardar dikes lie in the prolongation of the Abitibi dikes on a map of the reassembled Laurentia (Fig. 1). Together, they represent a fractured zone of > 2000 km in length (Ernst and Bell 1992). The Great Abitibi dike is strikingly similar in age, composition, and mineralogy to the Giant dike complexes of the Gardar Province. Moreover, olivine metagabbros in the Grenville Province, Ontario, were emplaced contemporaneously to late-Gardar activity at 1170 ± 30 Ma (Davidson and van Breemen 1988) and may, therefore, be related to the Gardar magmatism as well. The Aillik dikes in Labrador may also belong to this tectonomagmatic system and bridge the gap between the eastern end of the Abitibi swarm and the Gardar region because they are of the correct trend to support a continuation of the Abitibi swarm towards the Gardar region. The Aillik dikes are normally magnetized, as are the Abitibi dikes, and their pole position is concordant with those of the Abitibi dikes (Fahrig and Larochelle 1972), thus strengthening the link between the two dike swarms. They have a poorly defined inferred age of around 1100 Ma range based on K–Ar dates (Fahrig and Larochelle 1972). Other features also suggest a connection between magmatism in the Gardar Province and on the Canadian Shield (e.g., the contemporaneous emplacement of the Gardar BD_0 dikes (1280 ± 5 Ma, Upton et al. 2003) and the Harp (1273 Ma) and Nain LP dikes (1280–1277 Ma) on the Canadian Shield (Cadman et al. 1993; Buchan et al. 1996; Ernst and Buchan 2002)) and the occurrence of feldspathic inclusions in Gardar rocks likely related to the anorthosite formation on the Canadian Shield (Bridgwater 1967; Halama et al. 2002).

Petrography and sample selection

The EF basalts mainly contain plagioclase laths embedded in interstitial clinopyroxene as the major and apatite and Fe–Ti oxides as subordinate primary magmatic mineral phases. Olivine pseudomorphs occur in some samples and secondary alteration products, such as chlorite, Fe-talc, and carbonate, are fairly common. The majority of the EF samples analyzed here (eight) were selected on the basis of their low degree of alteration (Halama et al. 2003), and five additional samples slightly more altered were chosen to complete the data set for the upper lavas.

Three relatively fine grained olivine-bearing gabbroic dike samples (GM 1735, GM 1803, GD 39) of the Nunarssuit–Isortoq swarm are included in the present study. Major magmatic mineral phases are olivine, clinopyroxene, titanomagnetite with ilmenite exsolutions, and plagioclase. Other

Table 1. Major and trace element analysis of Eriksfjord Formation basalts and basement rocks of the Northern Border Zone.

	EF basalts					Basement		
Sample:	EF 169	EF 170	EF 171	EF 172	EF 167	GR 76	GR 77	GR 78
Unit:	UL	UL	UL	UL	UL	NBZ	NBZ	NBZ
Group:[a]	1b	1b	1b	1b	2			
Major oxides (wt.%)								
SiO_2	46.07	44.00	46.14	45.45	45.86	73.67	69.54	61.44
TiO_2	4.05	3.85	3.80	3.61	3.08	0.10	0.47	0.61
Al_2O_3	13.58	14.28	13.76	14.26	15.52	14.24	14.41	17.21
Fe_2O_3	17.68	17.18	16.45	15.77	15.40	0.94	2.99	5.80
MnO	0.19	0.27	0.20	0.35	0.20	0.02	0.03	0.08
MgO	3.45	4.65	3.78	4.04	5.60	0.09	0.67	1.64
CaO	6.31	7.03	6.15	6.74	7.27	0.69	1.83	4.91
Na_2O	4.52	3.44	4.13	4.05	3.48	4.26	3.49	4.26
K_2O	2.09	2.82	2.55	2.26	1.81	5.56	4.79	1.97
P_2O_5	1.64	1.58	1.59	1.74	1.27	0.05	0.14	0.23
LOI	0.32	0.49	0.84	1.03	1.06	0.23	0.84	0.83
Total	99.90	99.58	99.38	99.30	100.54	99.85	99.21	98.97
Mg#	31.7	39.2	35.3	37.9	46.4	21.3	38.2	43.9
Trace elements (ppm)								
Sc	29.4	27.4	28.5	28.8	22.7	0.93	3.9	9.1
Cr	5	5	5	4	31	6	14	18
Co	35.9	42.4	35.7	32.1	50.9	0.93	4.8	13.6
Ni	19	17	18	10	55	2.4	7.0	20
Zn	112	131	100	174	111	31	27	86
Rb	33.0	38.2	43.2	45.2	35.6	128	125	109
Sr	330	479	383	389	927	221	330	157
Zr	254	251	257	268	185	110	394	182
Sb	0.34	0.37	0.52	0.44	0.10	0.11	0.19	0.04
Cs	1.01	2.17	2.1	0.69	1.52	0.35	0.97	2.75
Ba	1759	1332	2079	1401	1571	595	1914	359
La	40.9	38.0	38.0	40.6	37.6	42.2	206	19.5
Ce	98.9	89.2	94.3	99.8	83.8	72.1	401	41.5
Nd	50.9	54.4	52.7	54.0	35.5	22.9	111	26.0
Sm	12.5	11.7	12.2	13.2	8.76	3.38	17.5	4.52
Eu	4.35	3.8	3.85	4.48	2.9	0.76	2.11	1.15
Tb	1.46	1.39	1.43	1.57	0.91	0.23	1.49	0.60
Yb	4.33	4.07	4.26	4.64	2.56	0.64	3.58	1.83
Hf	6.02	5.69	5.92	6.38	3.84	3.28	9.03	4.12
Ta	1.28	1.19	1.26	1.32	2.19	0.41	1.19	1.19
Th	1.35	1.27	1.34	1.43	1.97	16.42	43.60	3.60
U	0.70	0.52	0.43	0.46	0.56	2.11	2.35	0.79
Th/Ta	1.05	1.06	1.06	1.09	0.90	39.7	36.6	3.02
Ta/Hf	0.21	0.21	0.21	0.21	0.57	0.13	0.13	0.29

Note: EF, Eriksfjord Formation; UL, upper lavas; NBZ, Northern Border Zone; LOI, loss on ignition.

[a] See text for definition of the two geochemical groups.

samples from the Isortoq dikes are not included in this work because they represent cumulates, relatively differentiated magmas (MgO <3 wt.%), or have suffered significant crustal contamination ($\varepsilon_{Nd} < -4$).

Samples from the Abitibi dike swarm were previously investigated in a paleomagnetic study (Macouin et al. 2003) that yielded the characteristic paleomagnetic direction defined in the study by Ernst and Buchan (1993). The Abitibi

Table 2. Trace element (ppm) analyses of Eriksfjord Formation basalts and Isortoq dikes.

	EF basalts								Isortoq dikes		
Sample:	EF 024	EF 039	EF 059	EF 063	EF 072	EF 108	EF 168	EF 174	GD 39	GM 1735	GM 1803
Unit:	LL	LL	LL	LL	ML	ML	UL	UL			
Group:[a]	1b	1b	1b	1b	1b	1b	2	2	1b	1b	1b
Sc	27.2	26.0	29.7	25.7	24.3	27.3	20.8	23.1	23.8	20.0	23.7
Cr	104	59	116	86	78	52	32	18	70	50	42
Co	47.7	53.2	52.5	53.8	49.6	45.7	44.1	38.0	45.8	47.4	52.9
Ni	84	87	94	112	103	55	44	38	69	73	55
Zn	144	97	94	106	103	82	181	127	113	98	128
Rb	26.2	5.0	3.3	26.3	13.9	38.4	45.8	41.3	16.3	18.1	21.1
Sr	522	414	375	482	537	717	989	851	470	639	441
Zr	194	121	117	155	103	135	130	166	159	133	187
Sb	0.03	0.02	0.03	0.09	0.04	0.14	0.15	0.06	0.10	0.03	0.03
Cs	0.55	0.86	0.29	3.04	1.22	0.58	1.52	1.30	0.31	0.58	0.51
Ba	462	324	172	378	435	547	929	1233	647	819	537
La	17.4	11.4	10.5	15.9	3.27	12.6	33.5	37.2	16.6	17.5	14.1
Ce	40.9	28.4	26.7	37.2	23.4	31.7	74.3	83.9	40.1	41.0	33.3
Nd	22.5	16.8	17.2	23.2	15.3	20.3	34.3	45.3	21.9	21.4	32.0
Sm	5.72	4.48	4.60	5.16	3.96	5.42	7.89	8.82	6.02	5.68	5.52
Eu	1.88	1.71	1.73	1.86	1.78	2.04	2.77	3.09	2.25	2.12	2.17
Tb	0.81	0.66	0.70	0.74	0.53	0.78	0.81	0.93	0.80	0.67	0.78
Yb	2.78	2.31	2.55	2.65	1.76	2.62	1.99	2.48	2.69	2.11	2.72
Hf	4.54	2.97	3.18	3.78	2.45	3.31	3.35	4.12	4.27	3.24	4.46
Ta	0.71	0.55	0.57	0.58	0.46	0.66	1.97	2.30	0.86	0.62	0.96
Th	1.17	0.66	0.70	1.00	0.49	0.60	1.68	2.04	1.01	0.76	0.86
U	0.29	0.18	0.23	0.28	0.11	0.16	0.50	0.56	0.35	0.25	0.31
Th/Ta	1.66	1.19	1.23	1.71	1.06	0.91	0.85	0.89	1.18	1.23	0.90
Ta/Hf	0.16	0.19	0.18	0.15	0.19	0.20	0.59	0.56	0.20	0.19	0.22

Note: Major element analyses have already been published (see Halama et al. 2003, 2004). EF, Eriksfjord Formation; LL, lower lavas; ML, middle lavas; UL, upper lavas.

[a] See text for definition of the two geochemical groups.

samples are olivine-gabbros composed of plagioclase, augite, olivine, titanomagnetite, and ilmenite. Accessory minerals include alkali feldspar, apatite, and biotite (Condie et al. 1987; Ernst and Bell 1992). Latitude–longitude coordinates for the Abitibi samples are given in Appendix A.

Analytical techniques

Major element compositions were determined by inductively coupled plasma analysis – atomic emission spectroscopy (ICP–AES) at the Service d'Analyse des Roches et des Minéraux (SARM, Nancy, France) for EF basalts and at the Université d' Bretagne Occidentale (UBO, Brest, France) for Abitibi samples, following the method given in Cotten et al. (1995). Uncertainties are ≤ 2%, except for P_2O_5 where the uncertainty is < 10%. The uncertainties correspond to the 1σ relative standard deviation based on > 25 analyses of several geochemical reference materials (for details, see www.crpg.cnrs-nancy.fr/SARM/). Results for the BEN standard deviate from the recommended values by < 1% (Cotten et al. 1995). Analyses of previously analyzed samples are given in Halama et al. (2003, 2004).

Trace element concentrations were determined by instrumental neutron activation analysis (INAA) at the Centre d'Études Nucléaires de Saclay (CEN, France). About 100–150 mg of powdered sample were wrapped in aluminum foils, introduced into a Cd container, and irradiated under an epithermal neutron flux (OSIRIS nuclear reactor). Counting with high-resolution γ-spectrometers was carried out after ~8 d for isotopes with short half-lives (2–67 h) and after ~30 d for those with half-lives up to several months. Further details of the method are given in Joron et al. (1997). Detection limits for the various trace elements range from 0.5 ppb (Ta) to 1.5 ppm (Zr). Errors, based on repeated analysis of the geochemical standard BEN, are typically < 3.5%.

Major and trace element geochemistry

New whole-rock major and trace element analyses of EF lavas, Isortoq and Abitibi dikes, and NBZ basement samples are presented in Tables 1–3. The relatively low MgO contents (2.8–6.8 wt.%) show that neither the lavas nor the dikes represent primary mantle melts. Minor element contents are quite variable (e.g., TiO_2: 1.3–4.1 wt.%; P_2O_5: 0.15–0.75 wt.%) and increase with decreasing MgO con-

Fig. 3. Binary trace element diagrams of Gardar and Abitibi samples to show effects of fractionation and assimilation – fractional crystallization (AFC) processes. (*a*) Sc vs. Th, (*b*) Co vs. Th. Partition coefficients are from the compilation of Rollinson (1993). Solid line marks fractional crystallization (FC) of olivine. Dashed line marks FC of a low-pressure assemblage (50% plagioclase, 30% clinopyroxene, 20% olivine). Dotted line denotes an AFC process with $r = 0.6$ (r = rate of assimilation/rate of fractional crystallization), the low-pressure assemblage fractionating and an average of the three Northern Border Zone samples as assimilant. For all models, the most primitive Eriksfjord Formation (EF) basalt sample was used as initial composition. ol, olivine; cpx, clinopyroxene; plag, plagioclase; ◆, EF basalts, lower and middle lavas; ◇, EF basalts, upper lavas; ○, Abitibi dikes Groups 1a and 2; ■, assimilant for AFC modeling (average of three Northern Border Zone samples).

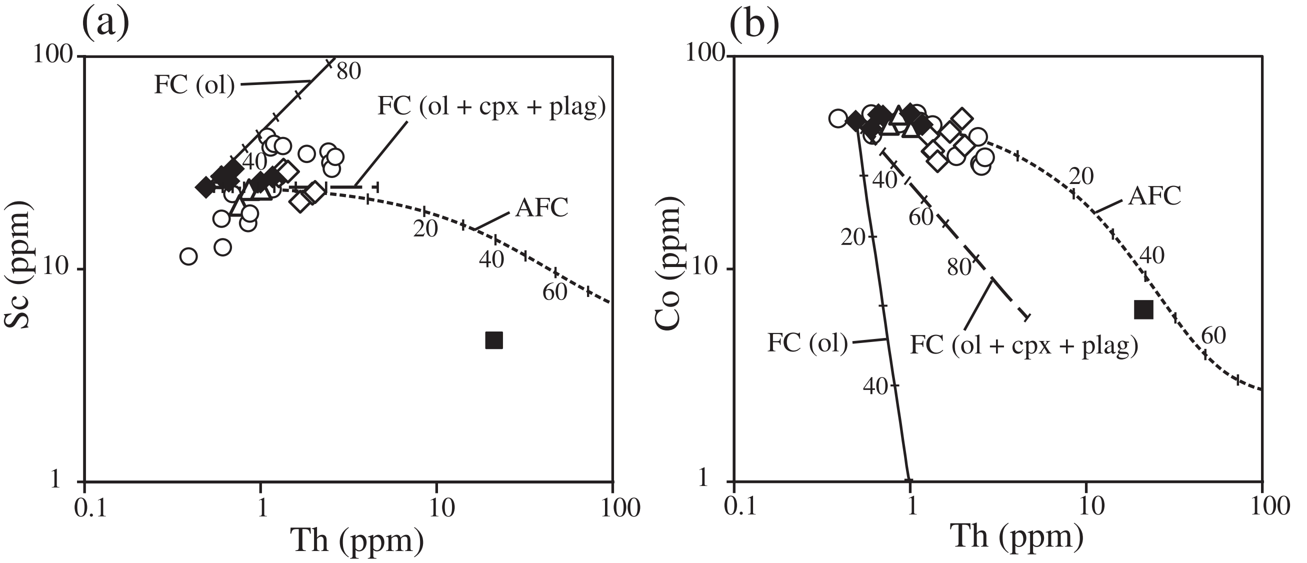

tents. A positive correlation of Ni with MgO and relatively low maximum Ni and Cr concentrations of 112 ppm and 176 ppm, respectively, are evidence for olivine fractionation (Fig. 2*a*). However, the relatively high Co (>30 ppm) and Sc contents (20–30 ppm for Gardar samples, 12–42 ppm for Abitibi samples) and the lack of a positive correlation between Sc and MgO indicate that no or only little clinopyroxene fractionation occurred (Fig. 2*b*). Thus, the rock compositions are still relatively primitive, especially with respect to some highly evolved Gardar igneous complexes. Ba and Rb show a positive correlation in the Abitibi rocks (Fig. 2*c*), consistent with their generally good correlation in basaltic rocks (Hofmann and White 1983). On the other hand, the significant scatter in the Gardar rocks suggests secondary mobility of Rb and (or) Ba. Sc–Th and Co–Th plots (Fig. 3) show that some of the compositional variation is consistent with both differences in the degree of partial melting as well as assimilation – fractional crystallization (AFC) processes, using a contaminant similar in composition to granitic gneiss from the NBZ. Fractional crystallization of olivine or a low-pressure assemblage (olivine + clinopyroxene + plagioclase) alone cannot explain the data because it would lead to significantly lower Co contents.

Primitive mantle-normalized trace element patterns (Fig. 4) were used to identify different geochemical groups. For the Abitibi dikes, two major groups can be distinguished. The first one shows a marked decrease from Cs to Ba and a relatively flat pattern from Ba to Yb with a small negative Sr anomaly (Fig. 4*a*). The second group is characterized by Ba peaks, Th–U and Zr–Hf troughs and elevated Ta and light rare-earth element (LREE) contents (Fig. 4*b*), features that were described as typical for magmas from the Great Abitibi dike (Ernst and Bell 1992). A subset of these samples has positive Sr anomalies and low Rb contents, but otherwise the trace element patterns are parallel.

Three samples from the EF upper lavas basalts are almost identical to the second group of Abitibi, both in absolute concentrations and patterns, except for slightly elevated Cs and Rb contents (Fig. 4*c*). Thus, a total of 11 Abitibi and three EF samples make up Group 2. For Group 1, the pattern of the Abitibi dikes is fairly similar to EF basalts from the lower and middle lavas and to the Isortoq dikes. However, there are also some notable differences, such as Ba peaks, low Cs and Rb contents relative to Ba, depletions of U and Th, and a slightly steeper slope from Zr to Yb in the Gardar rocks. Accordingly, Group 1 is subdivided into 1a (five Abitibi samples) and 1b (nine EF and three Isortoq samples).

Some of the variability of Cs, Rb, Ba, and Sr in the mantle-normalized trace element patterns may be caused by secondary alteration because these elements are prone to post-magmatic redistribution during burial metamorphism (Gibson et al. 1987); the mobility of Rb and (or) Ba in the Gardar rocks has been demonstrated earlier in the text (Fig. 2*c*). The consistent occurrence of the Ba peak compared with variable Rb abundances (Fig. 4*c*) suggests mobility of the latter. Ba enrichment relative to Rb may be related to the presence of interstitial alkali feldspar, which has been described in the Abitibi dikes (Ernst and Bell 1992). However, this explanation is unlikely because even the primitive samples that lack alkali feldspar show Ba peaks. Thus, the Ba enrichment is considered a feature of the mantle source. There was, however, no evidence found for the presence of phlogopite in the mantle source, based on several diagrams that might indicate its presence, such as Ba/Al_2O_3 and Sr/Al_2O_3 vs. Th (Johnson

Table 3. Major and trace element analysis of Abitibi dikes.

Sample:	Q204	Q205	Q206	Q207	Q209	Q7	T101	T103	T104	T108
Group:[a]	1a	1a	1a	1a	1a	2	2	2	2	2
Major oxides (wt.%)										
SiO_2	50.00			50.25	49.40	45.80	46.80		46.10	
TiO_2	2.16			1.32	1.37	3.48	2.50		2.40	
Al_2O_3	14.10			14.10	14.45	15.56	18.25		18.95	
Fe_2O_3	17.10			13.90	13.70	14.36	11.88		12.45	
MnO	0.23			0.20	0.20	0.19	0.15		0.15	
MgO	3.24			6.05	6.20	3.34	5.82		5.49	
CaO	7.60			10.10	10.20	9.68	9.50		9.00	
Na_2O	2.70			2.01	1.95	3.80	3.23		3.33	
K_2O	0.87			0.88	0.75	1.39	0.75		0.77	
P_2O_5	0.25			0.19	0.15	1.52	0.50		0.58	
LOI	1.25			0.83	1.18	0.22	–0.11		0.02	
Total	99.50			99.83	99.55	99.34	99.27		99.24	
Mg#	31.1			50.9	51.8	35.6	53.8		51.2	
Trace elements (ppm)										
Sc	35.8	38.9	42.0	38.0	37.4	34.9	22.6	18.3	16.5	12.7
Cr	5	149	176	120	171	2	29	45	77	13
Co	41.8	47.1	53.7	47.5	49.3	33.9	47.7	48.3	49.3	42.7
Ni	31	95	42	48	96	12	66	62	62	84
Zn	–	–	–	–	–	–	–	–	–	–
Rb	62.2	33.1	42.2	72.5	56.4	20.3	9.4	9.2	9.5	8.4
Sr	225	137	121	146	149	825	999	1026	1023	1208
Zr	163	95	83	99	79	169	61	61	72	57
Sb	0.10	0.36	0.07	0.03	0.04	0.03	0.02	0.02	0.02	0.02
Cs	3.95	3.83	4.77	4.93	4.61	0.58	0.67	0.47	0.87	0.50
Ba	168	105	98	141	127	1311	703	767	726	638
La	14.0	7.32	6.90	8.15	7.03	37.6	14.6	17.3	16.9	11.7
Ce	33.5	17.8	16.3	20.0	17.3	88.3	33.2	38.3	36.2	25.6
Nd	—	—	—	—	—	—	—	—	—	—
Sm	6.25	3.46	3.23	3.8	3.2	10.4	4.11	4.31	4.27	2.93
Eu	2.28	1.25	1.21	1.42	1.21	4.46	2.16	2.49	2.13	1.91
Tb	1.14	0.65	0.62	0.72	0.60	1.20	0.47	0.50	0.48	0.34
Yb	4.75	2.89	2.63	2.96	2.62	3.04	1.24	1.34	1.22	0.87
Hf	4.74	2.64	2.34	2.74	2.3	4.26	1.76	1.93	1.76	1.26
Ta	0.83	0.47	0.43	0.47	0.42	2.26	1.02	1.16	1.04	0.71
Th	2.43	1.19	1.09	1.34	1.14	1.83	0.69	0.87	0.85	0.61
U	0.62	0.31	0.31	0.34	0.28	0.42	0.17	0.21	0.20	0.14
Th/Ta	2.93	2.54	2.53	2.85	2.71	0.81	0.68	0.75	0.82	0.86
Ta/Hf	0.18	0.18	0.18	0.17	0.18	0.53	0.58	0.60	0.59	0.56

Note: LOI, loss on ignition.

[a] See text for definition of the two geochemical groups.

et al. 2005) (not shown). The small but distinct Sr peaks and troughs can be explained by variable degrees of plagioclase assimilation and (or) accumulation and fractionation, respectively, because Sr is compatible in plagioclase ($D_{Sr}^{plag\text{-}melt}$ = 1.5–2.8, Bindeman et al. 1998). This interpretation is consistent with a positive correlation between Sr and Al_2O_3 for the Abitibi Group 2 rocks (not shown).

Correlations among incompatible elements may also be used to identify cogenetic igneous rocks. Th is a useful indicator of the degree of partial melting because it is one of the most incompatible elements with mineral-melt partition coefficients for the major mantle phases below 0.01 (McKenzie and O'Nions 1991; Salters and Longhi 1999; Salters et al. 2002). High-field-strength elements (HFSE) are slightly less incompatible because they can be incorporated to a small extent into clinopyroxene and garnet (e.g., $D_{Hf}^{cpx\text{-}melt}$ = 0.049–0.344, Salters and Longhi 1999). The Sm–Ta and Hf–Ta diagrams (Fig. 5) exemplify the broad division into two distinct

Table 3 (*concluded*).

T203	T207	T208	T301	T306	T310
2	2	2	2	2	2
48.25	46.50			47.20	45.70
3.11	3.63			1.70	2.99
14.10	13.00			20.75	17.60
15.10	17.00			10.08	12.80
0.21	0.24			0.12	0.16
2.83	3.00			6.40	5.17
7.90	8.04			9.27	8.95
4.38	4.00			3.26	3.30
1.79	1.78			0.48	0.88
1.40	1.75			0.26	0.72
0.22	0.37			–0.19	1.08
99.29	99.31			99.33	99.35
30.8	29.6			60.1	49.0
31.7	33.8	29.7	17.3	11.5	23.8
5	5	5	16	9	17
31.3	33.5	30.5	53.5	51	46.1
6.1	3.7	3.4	91	84	75
–	–	–	–	–	–
28.1	26.2	25.8	6.5	4.6	14.3
777	708	730	1070	1142	882
181	182	179	46	40	109
0.03	0.11	0.03	0.08	0.02	0.10
0.56	0.39	0.42	0.39	0.30	1.57
1737	1759	1932	631	518	848
43.9	51.4	44.2	11.9	8.37	21.4
97.6	118	99.2	26.8	18.4	49.4
—	—	—	—	—	—
11.9	14.1	11.76	3.18	2.10	5.63
5.27	5.36	5.56	2.07	1.51	2.48
1.32	1.55	1.33	0.37	0.23	0.64
3.44	3.85	3.58	0.94	0.61	1.71
4.98	5.18	5.03	1.32	0.90	2.49
2.42	2.87	2.53	0.77	0.57	1.40
2.49	2.66	2.54	0.60	0.39	1.17
0.62	0.70	0.72	0.16	0.10	0.29
1.03	0.93	1.00	0.78	0.68	0.84
0.49	0.55	0.50	0.58	0.63	0.56

geochemical groups established based on the normalized trace element diagrams. Modeled curves for fractional crystallization and AFC show that neither process can explain the difference in slopes between the two trends. The fractionating assemblage (50% plagioclase, 30% clinopyroxene, 20% olivine) used for calculating the models reflects low-pressure crystallization of basaltic magmas, but changes in the proportions of fractionating phases do not significantly change the models because bulk partition coefficients of the elements chosen are generally too low in basaltic systems to generate substantial fractionation (McKenzie and O'Nions 1991; Kelemen et al. 1993; Bindeman et al. 1998; Salters et al. 2002). Moreover, it was shown before (Fig. 2) that clinopyroxene, the only phase that may incorporate minor amounts of HFSE, has not been significantly fractionated. The choice of the assimilant is based on the feasibility to explain Sr–Nd isotope trends by crustal contamination, using this gneissic material from the NBZ (Halama et al. 2004). The difference in slope between Groups 1 and 2 indicates that different source chemistries must be involved in the generation of the two trends.

A more systematic evaluation of various other binary diagrams of incompatible trace element pairs (Fig. 6) reveals that Group 2 samples always define a clear linear trend for all incompatible element pairs investigated (e.g., Zr–Ta, Sm–Hf, Yb–Th). On the other hand, the characteristics of Groups 1a and 1b are less well defined, and the trends generally exhibit more scatter (e.g., U–Ta, Ta–Th). As for the Sm–Ta and Hf–Ta diagrams, Group 1 samples as a whole may show a coherent trend distinct from Group 2 samples (e.g., Zr–Ta). They may also form a trend close to the one of Group 2 (e.g., Sm–Hf), or they may exhibit distinct trends of the two subgroups 1a and 1b (e.g., Hf–Th, Yb–Hf).

Discussion

Evidence for distinct mantle sources

Binary diagrams of incompatible trace element ratios (e.g., Th/Ta vs. Th/Tb) in primitive rocks may be used to distinguish fractionation effects owing to partial melting from source heterogeneities (Joron and Treuil 1989). Because these ratios might also be affected by crustal contamination (Condie 2003) and by crystal fractionation, the influence of both processes must be evaluated first, using MgO content and ε_{Nd} values as respective geochemical indicators (Fig. 7). Measured incompatible trace element ratios are not dependant on MgO contents, suggesting that crystallization of olivine and cotectic minerals did not significantly fractionate these elements. Calculating the effects of fractional crystallization on the trace element ratios investigated reveals that changes in the ratios are indeed very small. For instance, the change in Th/Tb is ~7% after 50% of crystallization, which is smaller than the symbol size used in the figure. This is in agreement with low partition coefficients for incompatible elements, particularly in olivine (Kelemen et al. 1993; Salters et al. 2002), and the generally insignificant effects of low-pressure crystal fractionation on incompatible trace element ratios (Weaver et al. 1986). The negative ε_{Nd} values of some Group 1 rocks are thought to reflect minor assimilation (<5%–10%) of lower crustal material (Halama et al. 2004). However, the trace element ratios used here are not significantly changed by the contamination and the two distinct groups can be distinguished independently of the degree of contamination (Figs. 7*c*, 7*d*). In summary, the influence of FC and AFC processes on the trace element ratios used to investigate the mantle sources is negligible.

Two distinct trends can be recognized on the Th/Ta vs. Th/Hf and Th/Ta vs. Th/Tb diagrams (Figs. 8*a*, 8*b*). Care must be taken because the use of ratio–ratio plots with a common element in both ratios can cause spurious correlations (Rollinson 1993). However, because the two geochemical groups were previously identified on mantle-normalized and binary trace element diagrams (Figs. 4–6), it is likely that the correlations do not correspond to artifacts. Thus, the observed trends are interpreted as batch partial melting trends from two geochemically distinct sources (Joron and Treuil 1989). Both trends include samples from both the Gardar Province and the Abitibi dike swarm. For the EF basalts, heterogeneous sources have only been involved in the late stages of the eruptive history because all the lower and middle lava samples belong to the Group 1 trend.

In summary, the geochemical features suggest that the two groups of magmas defined earlier in the text are not produced by different degrees of partial melting of a common mantle source or by fractional crystallization of common parent magma. The existence of two distinct sources for the EF basalts has already been suggested on the basis of REE patterns in clinopyroxene and oxygen isotope data (Halama et al. 2003). The Th/Ta–Ta/Hf diagram (Fig. 8*c*) may be used to relate the two mantle components identified to known mantle reservoirs, based on a large trace element database of MORB and OIB (Joron and Treuil 1989; Joron 2000; Joron, unpublished data). Group 1a and 1b samples are characterized by Ta/Hf ~0.2 and plot between DMM and the OIB field. The slight variability in Th/Ta is consistent with differences in the degree of partial melting. Group 2 samples show significantly elevated Ta/Hf ratios between 0.5 and 0.7, plotting into the OIB field. Mixing between the source components of Group 1 and 2 appears to be of minor importance.

Magma generation

The melting pressures and the extent of partial melting of mantle sources may be traced using REE patterns because they are strongly dependent on the degree of partial melting and the nature of the aluminous phase (spinel or garnet) in the source (Reichow et al. 2005). Specific REE ratios such as Ce_N/Yb_N may also be used as indicators of crustal contamination (Reichow et al. 2005), but this effect has been shown to be insignificant in our sample set (Fig. 7).

Group 2 samples show higher Ce_N/Yb_N and Tb_N/Yb_N ratios than the Group 1 samples (Fig. 9). This suggests that either the source of Group 2 is more enriched in LREE or the Group 2 magmas formed at lower degrees of partial melting of a chemically relatively homogeneous source. Qualitatively, the relatively strong fractionation of the heavyREEs with $Tb_N/Yb_N > 1.5$ in Group 2 indicates that these magmas formed in the presence of garnet. For quantification, partial melting is modeled using source compositions representing different degrees of enrichment. Positive ε_{Nd} values in some EF lavas (Paslick et al. 1993) suggest that the mantle source has been moderately depleted for a long period of time. However, DMM is not considered to be a major source component for both Abitibi (Ernst and Hattori 1992) and primitive Gardar rocks (Halama et al. 2003). Consequently, model source compositions were determined by re-enriching DMM with a partial melt derived from this source. Such enriched sources may originate by metasomatism involving small-degree melts (Hawkesworth et al. 1984) or by mixing depleted peridotite with subducted material (Hofmann and White 1982), and similar source compositions have been successfully used in modeling intraplate magma generation (Haase et al. 2004). The primitive mantle composition is not used for modeling because geophysical, geodynamical and geochemical observations suggest the lack of preservation of primitive mantle (Van Keken et al. 2003). Source composition M1 was calculated by mixing 10% of a 5% partial melt to DMM. It is considered as a relatively LREE-depleted end-member mantle component, consistent with slightly positive ε_{Nd} values for EF middle lavas (Paslick et al. 1993). M2 has been re-enriched by 25% mixing with a 5% partial melt from the DMM. Finally, Z-35 is a metasomatically enriched natural peridotite from Zabargad Island, Red Sea, Egypt (Bonatti et al. 1986).

The Abitibi rocks of Group 1a can be modeled by 8%–20% melting of a M1 source in the spinel facies. The lower and middle lavas from the EF basalts plot just below ~20%–30% melting of the same source in the garnet facies. The upper lavas of Group 1b can be modeled by 12%–14% melting of the same source in the garnet facies. Compositions of the Group 2 samples fall slightly above the 15%–20% melting interval of a M2 source in the garnet facies. Using the more enriched Z-35 (Bonatti et al. 1986) as source, the Group 2 samples can be modeled by 20%–30% melting. Given the selectivity of the models to the selected garnet-liquid partition coefficients and the occurrence of garnet in source and melting mode, the misfit could be compensated by subtle changes in these parameters. We suggest, however, that enriched mantle sources as represented by M2 and Z-35 are mainly involved in the generation of the Group 2 samples.

The moderate degrees of melting obtained from modeling (~10%–30%) compare well with degrees of melting determined for other dikes (Scourie dikes: 20%, Tarney and Weaver 1987; Proterozoic dikes of the Superior Province: 5%–25%, Condie et al. 1987) and basalts (West Siberian basalts: 10%–20%, Reichow et al. 2005). The important point here is that it is not possible to model the Group 2 compositions using melts produced in the spinel facies, indicating the presence of garnet in the source of the Group 2 samples. This is consistent with the occurrence of metasomatized and originally possibly garnetiferous mantle-derived peridotite xenoliths in Tugtutôq–Ilímaussaq dikes (Upton 1991). Magma generation of the Group 2 magmas is, therefore, inferred to have occurred at depths > 70–80 km, where the transition from spinel to garnet peridotite takes place (Green and Ringwood 1967; Robinson and Wood 1998). The trend of the Group 1 data might reflect varying proportions of melts derived from a garnet-bearing source (Bernstein et al. 1998), but a predominant derivation from beneath thinned continental lithosphere in the spinel facies during intense crustal extension is indicated (Ellam 1992). It is also evident that for all samples an addition of incompatible elements in the source relative to DMM is required, except perhaps for the Group 1a samples.

Geochemical characteristics of the mantle sources

The available geochemical data provide a basis for evaluating the contribution of different mantle components to the Gardar–Abitibi magmatism. The geochemical groups identified by using trace elements display only small differences in their Nd isotopic signatures (Figs. 7*c*, 7*d*). The ε_{Nd}(i) value of the isotopically most depleted sample from Group 1

Fig. 4. Trace element concentrations of selected Gardar and Abitibi samples normalized to primitive mantle values (McDonough and Sun 1995). (*a*) Abitibi dikes, Group 1a. The grey field represents the Eriksfjord Formation and Isortoq samples defining Group 1b. (*b*) Abitibi dikes, Group 2. (*c*) Eriksfjord Formation basalts. The grey field represents the Group 2 Abitibi dikes without the positive Sr anomaly. (*d*) Isortoq dikes. The grey field represents the 1170 ± 30 Ma metagabbros from the Grenville Province (R.E. Ernst, unpublished data, on samples from A. Davidson).

(a) Abitibi dikes - Group 1a

(b) Abitibi dikes - Group 2

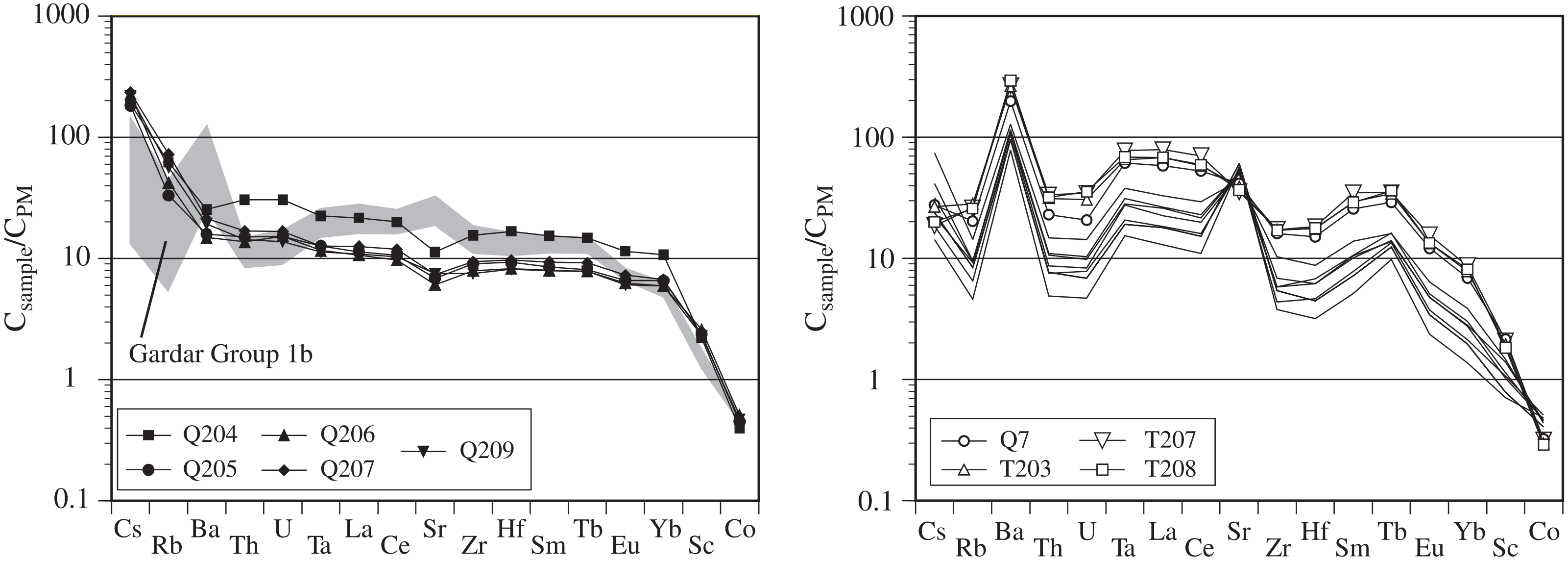

(c) Eriksfjord formation basalts

(d) Isortoq dikes

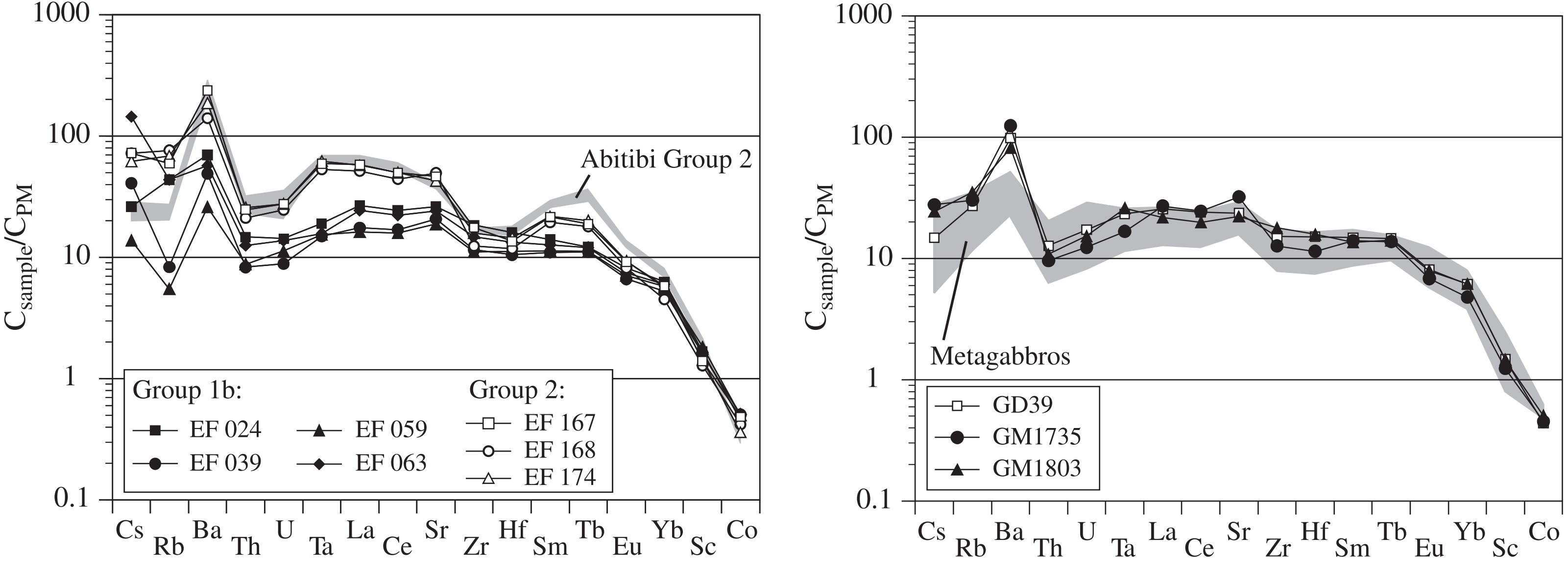

Fig. 5. Distinction of Group 1 and 2 samples based on (*a*) Sm vs. Ta, and (*b*) Hf vs. Ta. The dashed line marks fractional crystallization (FC) of a low-pressure assemblage (50% plagioclase, 30% clinopyroxene, 20% olivine). The dotted line denotes an assimilation – fractional crystallization (AFC) process with $r = 0.6$ (r = rate of assimilation/rate of fractional crystallization), the low-pressure assemblage fractionating and an average of the three Northern Border Zone samples as assimilant. For all models, the most primitive Eriksfjord Formation (EF) basalt sample was used as initial composition. Partition coefficients (D values) used are from the compilations of McKenzie and O'Nions (1991) for Th and Sm and Halliday et al. (1995) for Hf. D_{Ta} values were assumed to be similar to the D_{Nb} values given in McKenzie and O'Nions (1991). ◆, EF basalts, lower and middle lavas; ◇, EF basalts, upper lavas; △, Isortoq dikes; ⭘, Abitibi dikes, Group 1a; ○, Abitibi dikes, Group 2; ■, assimilant for AFC modeling (average of three Northern Border Zone samples). Errors are smaller than the symbol size.

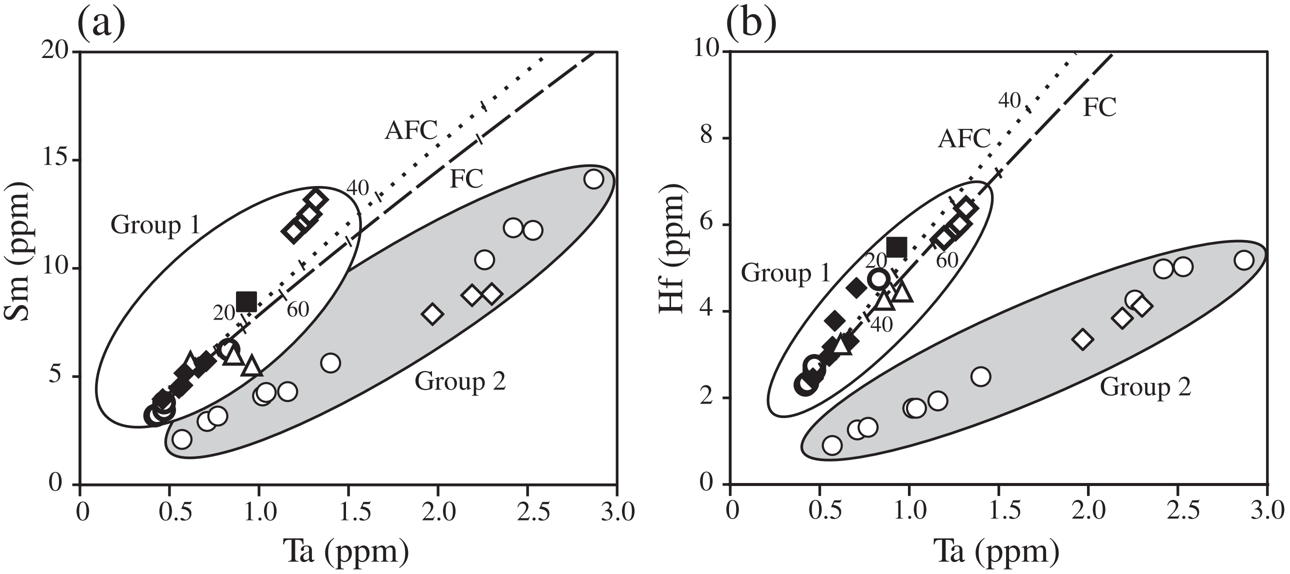

is similar to initial ε_{Nd} values from isochrons for the EF basalts ($\varepsilon_{Nd}(i) = +2.2$ and $+2.3$, respectively, Paslick et al. 1993). This suggests a mantle source slightly depleted in incompatible elements. However, Group 1 rocks are enriched in trace element contents relative to the primitive mantle, suggesting that the trace element enrichment occurred only shortly before the magma generation event. Decoupling of trace elements and isotopic ratios is quite common and indicate enrichment processes that have operated over varying time scales (Okamura et al. 2005). ε_{Nd} values around 0, which are typical for Group 2 rocks, are interpreted as a mixture among different mantle components. This is in agreement with Nd isotopic data ($\varepsilon_{Nd} = 0$) from East African carbonatites that have been explained as a mixture of the HIMU and EM1 mantle components (Bell and Simonetti 1996). They may also include a FOZO-type component, but this is difficult to evaluate because the composition of FOZO in the Proterozoic is not known.

Group 2 shows incompatible trace element patterns with OIB characteristics, such as a relative Ta enrichment, an overall decrease in enrichment in REE and HFSE abundances, and elevated Ta/Hf ratios. These features were previously also recognized for the Great Abitibi dike, and a derivation from an incompatible element-enriched mantle similar to the source for OIB was proposed (Ernst and Bell 1992). However, trace element patterns of Gardar basaltic magmas were described as consistently different from those of OIB, and their source accordingly attributed to a lithospheric mantle that was mildly enriched relative to MORB (Upton et al. 2003). Following Condie (2005), we use HFSE ratios to discriminate between the primitive mantle, DMM, and mantle sources that include recycled components (HIMU, EM1, and EM2). The trace element data that were chosen to represent the end-member mantle components were taken from ocean islands that show the respective geochemical signatures most strongly (HIMU: Austral-Cook Islands, Chauvel et al. 1992; Hauri and Hart 1997; EM1: Kerguelen, Frey et al. 2000; EM2: Samoa, Workman et al. 2004). The comparison of mantle source components from oceanic regions with continental magmatism is justified because the oceanic mantle components are also found in intraplate magmatism (Nelson et al. 1988; Franz et al. 1999; Cook et al. 2005). The data show that DMM was no major source component of the magmas (Fig. 10), in agreement with isotope data (Halama et al. 2003). Group 1 samples show only limited overlap with any of the sources involving recycled components. It may be interpreted as a source dominated by an isotopically depleted mantle component that experienced trace element enrichment just prior to magmatism. Because Group 1 samples plot close to or in prolongation of the fields for EM1 (Fig. 10), the trace element enrichment may be related to an EM1-type source contribution. The enrichment can be envisaged as produced by infiltration of astenospheric partial melts that were stored in the mantle lithosphere. Melting would have been triggered by progressing extension, and the resulting melts would incorporate both astenospheric material and parts of the previously enriched lithosphere. In later stages of magmatic activity when Group 2 rocks were produced, melting started at deeper levels and involved more enriched parts of the upwelling astenosphere. Group 2 samples exhibit considerable overlap with the EM2 field and plot close to the HIMU and EM1

Fig. 6. Binary diagrams of incompatible trace element pairs. The grey fields encompass all samples of Group 2. Symbols as in Fig. 5.

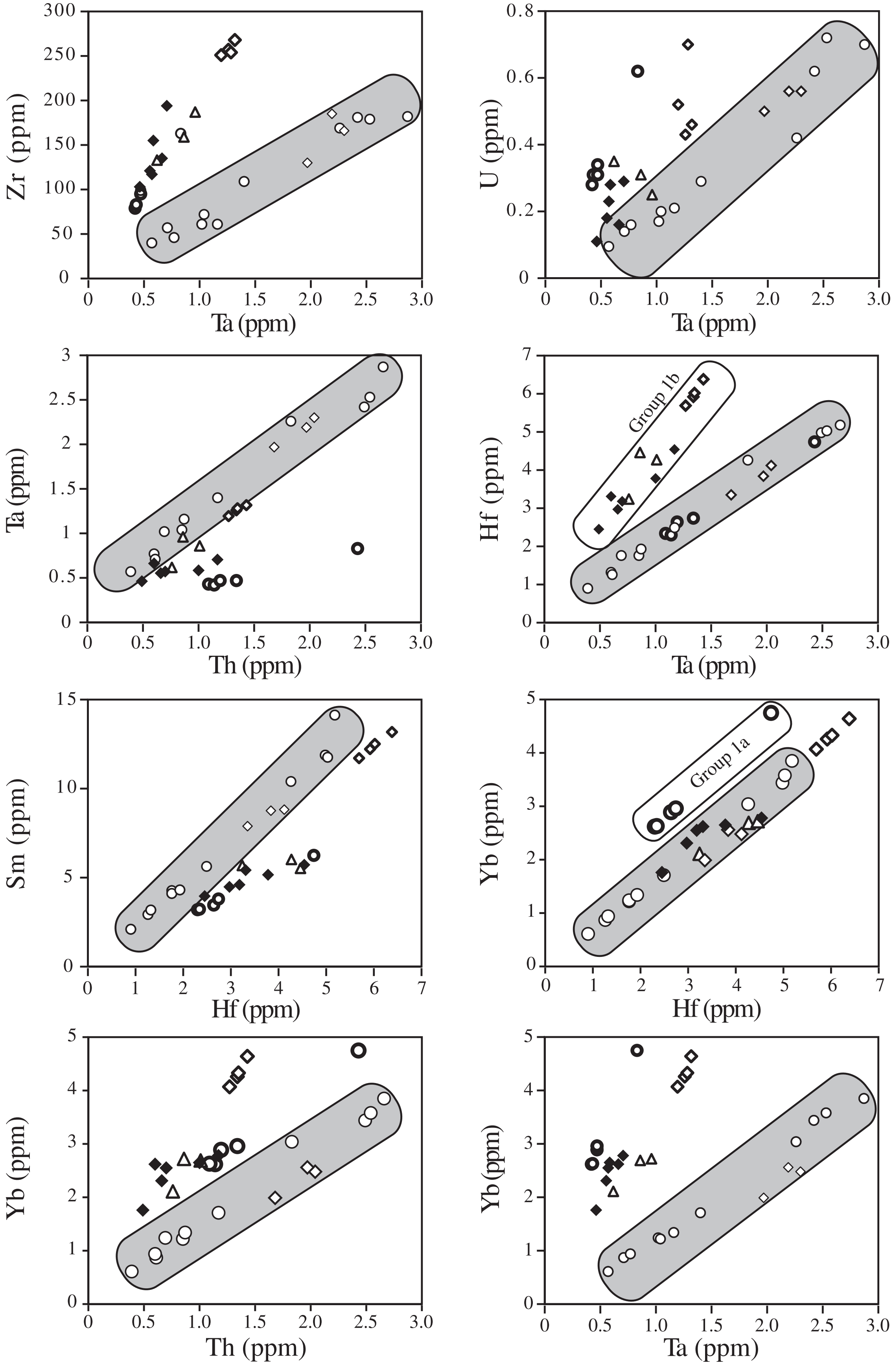

Fig. 7. Various trace element ratios used in deciphering the mantle source geochemical characteristics plotted against MgO (*a*, *b*) as indicator of magmatic differentiation and ε_{Nd} (*c*, *d*) as indicator of crustal contamination. ε_{Nd} values for Gardar rocks are from Halama et al. (2003, 2004). The ε_{Nd} value of Great Abitibi dike rocks is from Ernst and Hattori (1992), who give an average ε_{Nd} of –1 ± 0.5 for six samples. Ta/Hf is from Ernst and Bell (1992), and Ce_N/Yb_N is an average of 30 Abitibi dike samples from R.E. Ernst (unpublished data). Symbols as in Fig. 5.

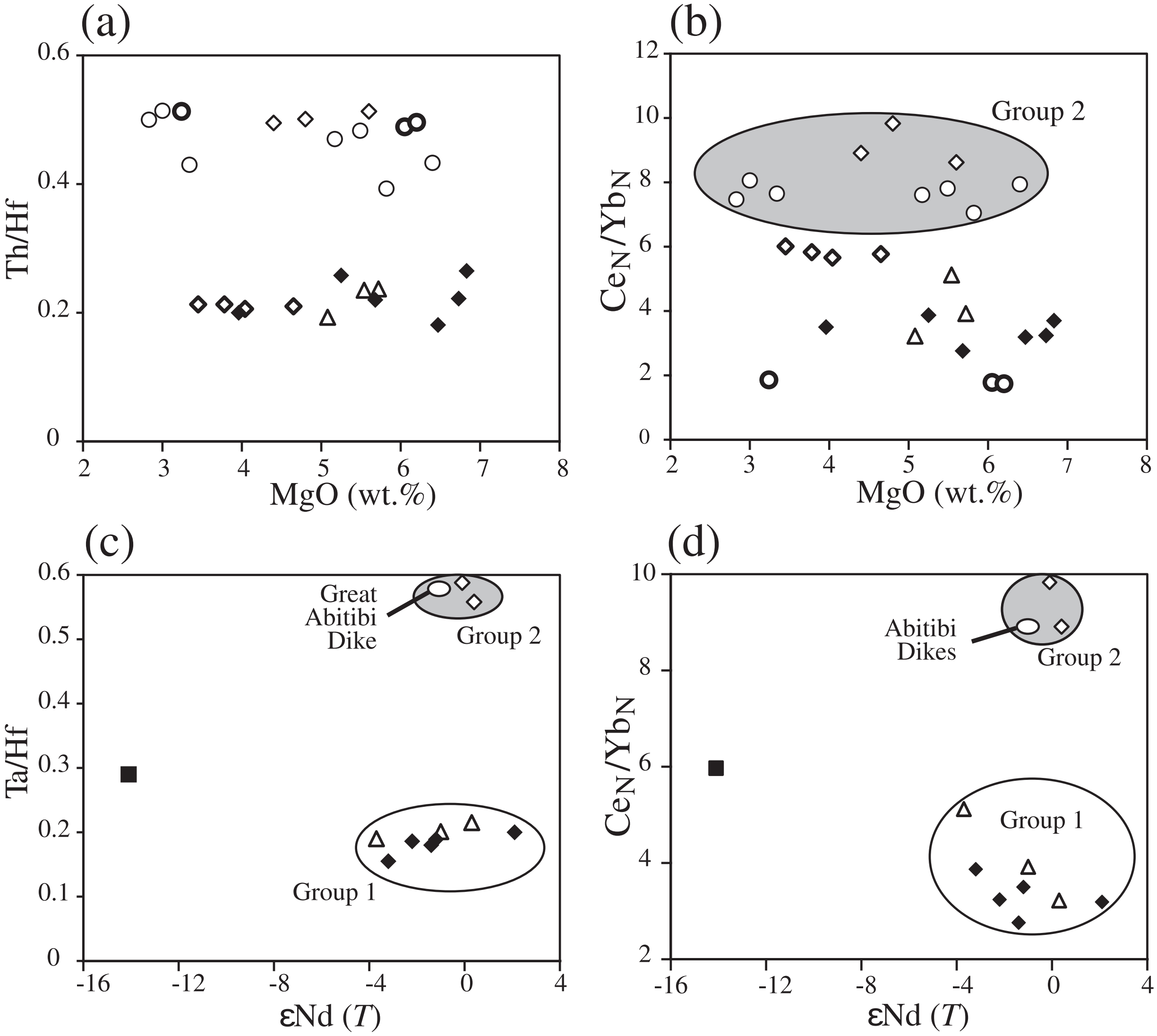

components as well. Although an assignment to a particular component is not possible, it is evident that they have many geochemical similarities with rocks derived from OIB-type sources and may include a FOZO-type astenospheric mantle component (Okamura et al. 2005).

Timing of events

The age of 1185 ± 22 Ma for a giant dike from the Nunarssuit–Isortoq swarm (Engell and Pedersen 1974), consistent with crosscutting relationships with the Nunarssuit syenite (1171 ± 5 Ma, Finch et al. 2001), suggests that Gardar Group 1 rocks are older than 1170 Ma. The age of the Abitibi Group 1 rocks is not known, but it is possible that the Abitibi dike chemistry reflects an age range, with Group 2 rocks (including the Great Abitibi dike emplaced at 1141 Ma) that is somewhat younger than the Group 1 rocks. In this respect, it is noteworthy that late Gardar dikes from the Tugtutôq–Ilímaussaq lineament, emplaced at ~1163 Ma (Buchan et al. 2001), have OIB-like trace element features based on the Ce/Y vs. Zr/Nb diagram that are distinct from the slightly older Isortoq dikes (Upton et al. 2003). La/Yb ratios in late Gardar dikes from Tugtutôq range from 11 to 19, and LREE and Nb are significantly enriched in the interval separating the eruption of the EF lavas and intrusion of the Giant dikes (Upton et al. 2003). Our data show that the youngest EF lavas (Group 2) are also enriched in LREE, similar to the Tugtutôq Giant dikes. This suggests that they were emplaced contemporaneously at around 1163 Ma. Because the Gardar Group 2 rocks are older than 1160 Ma, based on cross-cutting relationships with the 1160 Ma old Ilimaussaq intrusion (Krumrei et al. 2006), there is a distinct time gap to the emplacement of the Great Abitibi dike of ~20 Ma. Igneous rocks with geochemical characteristics of the Group 2, therefore, span an age range of at least 20 Ma,

Fig. 8. Binary diagrams of incompatible trace element ratios used to identify mantle sources. (*a*) Th/Ta vs. Th/Hf, (*b*) Th/Ta vs. Th/Tb, (*c*) Th/Ta vs. Ta/Hf. Composition of the depleted mid-ocean ridge basalt mantle (DMM) is after Workman and Hart (2005). The dashed arrow in (*a*) shows the theoretical partial melting trend of a source X. The dark grey field represents metagabbros from the Grenville Province (R.E. Ernst, unpublished data, on samples from A. Davidson). Data from the Aillik dikes are added for comparison (R.E. Ernst, unpublished data, on archival samples from W.F. Fahrig). Symbols as in Fig. 5. Three additional data points (●) are samples from the Great Abitibi dike, published by Ernst and Bell (1992). The generalized fields (bold outlines) of normal mid-ocean ridge basalt (N-MORB) and ocean-island basalt (OIB) in (*c*) are based on data from J.L. Joron (2000, unpublished data).

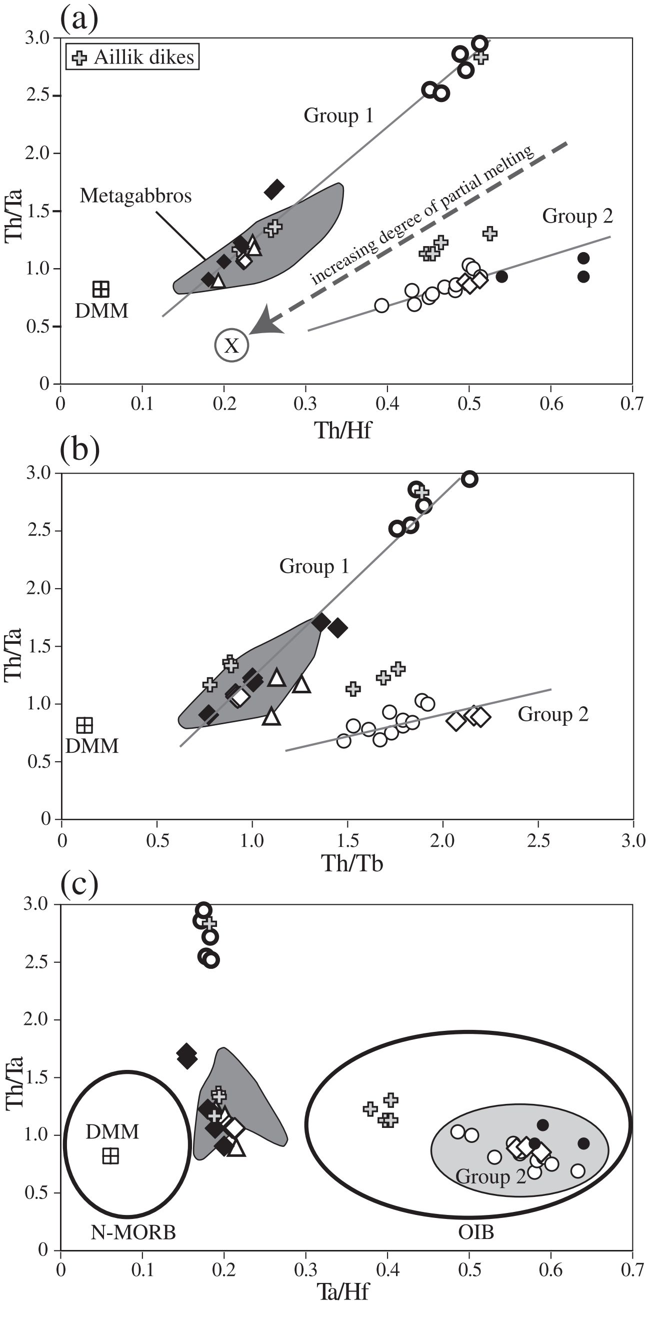

but the Abitibi and Gardar dikes do probably not reflect a single swarm because of the age differences.

A comparison with spatially and temporally related igneous rocks from the Canadian Shield reveals some additional geochemical similarities. The 1170 ± 30 Ma old metagabbros from the Grenville Province (Davidson and van Breemen 1988) show a remarkable similarity to Group 1b rocks (Figs. 4*d*, 8). Their emplacement age overlaps with those of the EF lavas and the Isortoq dikes, so a genetic relationship appears likely. The aforementioned Aillik dikes in Labrador appear to possess two distinct geochemical signatures: one very similar to Group 1 rocks and the other compositionally close to the Group 2 rocks. Unfortunately, their age is poorly constrained, but the overlap in the geochemical data with the Gardar and Abitibi rocks lends support to the idea that they are related to that magmatic activity.

Involvement of a mantle plume?

Because DMM is no major source component of the Gardar–Abitibi magmas, it seems likely that the enrichment of trace elements in the source may have been associated with upwelling of an astenospheric plume and (or) enriched subcontinental lithosphere (Paces and Bell 1989). It is commonly assumed that OIB is derived from chemically anomalous mantle sources associated with mantle plume activity (Weaver et al. 1986; Hofmann 1997, 2003) and OIB geochemical signatures in intracontinental magmatic rocks are, therefore, related to plume-related magmatism as well (Barrat et al. 1990; Bernstein et al. 1998). Coulson et al. (2003) noted that Gardar carbonatites and lamprophyres have geochemical and isotopic signatures that are similar to those typically found in OIB and, therefore, proposed an ultimate source in the astenospheric mantle. The deep formation of Group 2 magmas in the garnet peridotite stability field supports a plume origin (Haase et al. 2004). The trend of the data in Tb_N/Yb_N vs. Ce_N/Yb_N space could reflect the presence of varying proportions of melts from a garnet-bearing source, and melts with the highest Tb/Yb ratios should represent the melts with the highest proportion of a plume component (Bernstein et al. 1998).

The two distinct mantle sources identified may both be associated with a heterogeneous plume because lateral spreading and entraining of depleted mantle can occur in association with stalling of a rising plume at intramantle boundaries (Kempton et al. 2000). Group 1 rocks can be interpreted as dominated by depleted plume material, with minor trace element enrichment caused by either enriched streaks within the plume (Kerr et al. 1995) or the lithospheric mantle that has been enriched by astenospheric partial melts prior to eruption. The transition towards more OIB-like source characteristics in both the EF basalts and the dike swarms (Group 2 rocks) may be interpreted as an increasing contribution of more enriched material from the heterogeneous plume. A link between Gardar and Abitibi magmatism appears also feasible considering that sills and lava flows associated with plume heads can be emplaced as far as 2500 km away from the plume center by lateral injection (Ernst and Buchan 2001) or by long-distance lateral transport of plume material as sheets within astenosphere (Sleep 1997). The time gap between the late Gardar activity and the emplacement of the Abitibi dikes is consistent with a plume consist-

Fig. 9. Tb_N/Yb_N vs. Ce_N/Yb_N diagram for the Gardar and Abitibi mafic rocks. The curves show non-modal batch partial melting models of various mantle sources. M1 is a slightly re-enriched source (depleted mid-ocean ridge basalt mantle (DMM) source mixed with 10% of a 5% melt from the DMM), M2 is a moderately re-enriched source (DMM source mixed with 25% of a 5% melt) and Z-35 is a natural, metasomatically enriched peridotite from Zabargad Island, Red Sea, Egypt (Bonatti et al. 1986). Symbols are as in Fig. 2. Solid and dashed lines mark partial melting curves of M1 and M2, respectively, one each for spinel- and garnet-facies melting. The dotted line denotes melting of Z-35. Tick marks at the melting curves are at 1%, 2%, 4%, 6%, 8%, 10%, 15%, 20%, and 30% partial melting, if not noted otherwise. Concentration values for DMM and source mode spinel facies (57% olivine + 28% orthopyroxene + 13% clinopyroxene + 2% spinel) are after Workman and Hart (2005). Source mode garnet facies (54% olivine + 17% orthopyroxene + 9% clinopyroxene + 20% garnet) and melting modes (spinel facies: –0.44 olivne + 0.55 orthopyroxene + 0.67 clinopyroxene + 0.22 spinel; garnet facies: 0.1 olivine + 0.18 orthopyroxene + 0.3 clinopyroxene + 0.42 garnet) are after Kelemen et al. (1992). Batch melting equations are from Shaw (1970). All partition coefficients are from Kelemen et al. (1993), with values for Tb interpolated between Gd and Dy. all partition coefficients are assumed to be constant over the calculated melting regime for simplicity.

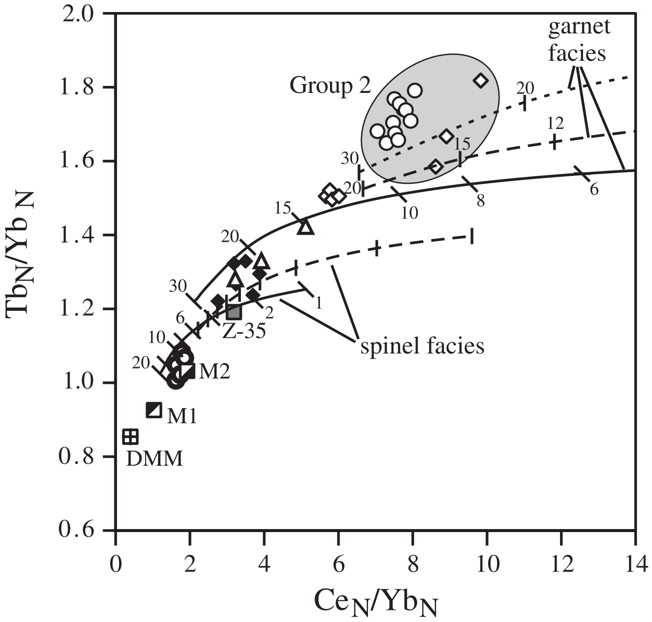

ing of several separate blobs rather than being continuous (Cadman et al. 1993; Haase et al. 2004). We envisage a pulsing plume with magmatic activity occurring in discrete phases, similar to models of the Iceland plume (O'Connor et al. 2000; Ito 2001). The first activity occurred around 1190–1170 Ma, leading to emplacement of the Isortoq dikes and the lower and middle Eriksfjord lavas in Greenland, and possibly some of the older Abitibi dikes and olivine gabbros, now metamorphosed, in Canada. A second pulse at around 1165–1160 Ma formed the Giant dikes of the Tugtutôq–Ilimaussaq swarm. Activity in the Gardar Province continued intermittently with emplacement of intrusive complexes (Ilimaussaq at 1160 ± 5 Ma, Østfjordsdal at 1147.5 ± 3.2 Ma, Paatusoq at 1144 ± 1 Ma; Upton et al. 2003). A third major pulse producing more mafic magmas was focused in the Abitibi area, and dikes were emplaced along zones of lithospheric weakness. Later pulses forming the Aillik dikes might be related to another pulse of that same plume, in a way similar to the pulsing of the Iceland plume over the last 70 million years (O'Connor et al. 2000). This scenario is consistent with models of thermochemical instabilities in plumes that can cause magmatic activity in episodes with time gaps of several million years (Lin and van Keken 2005).

The recurrent activity in the whole region (1.28 and 1.20–1.14 Ga in the Gardar Province, Upton et al. 2003; 1.14 Ga for the Abitibi dikes, Krogh et al. 1987; 1.11–1.08 Ga for the Keweenawan Rift, Davis and Paces 1990) could be related to a long-lived superplume, as proposed for the protracted magmatism in Siberia at ~350 Ma, 250 Ma, and in the Cenozoic (Yarmoluk et al. 2000). The presence of a periodically active superplume also presents an alternative explanation for the recurrent production over some 200 Ma of rocks with close petrographical and geochemical similarities, which has been explained by a uniform, nonconvecting reservoir in the lithospheric mantle (Upton et al. 2003).

Conclusions

Two geochemically distinct mantle sources are identified for the basaltic rocks of the Late Gardar (1.20–1.14) activity in the Gardar Province, South Greenland. Both sources are variably enriched in incompatible trace elements compared with DMM. One source shows trace element features similar to OIB-type sources and modeling of partial melting indicates that garnet was present in the source. These features suggest the involvement of a mid-Proterozoic mantle plume in the later stages of the Gardar magmatism. The proposed plume influence is also consistent with isotopic evidence for the associated Midcontinental Rift magmatism that indicates a plume component (Nicholson et al. 1997) and the presence of giant dike swarms (Ernst and Buchan 1997). The origin of the second source is less well defined, but its composition corresponds to a source slightly depleted relative to the OIB-type plume source. It is interpreted to involve a depleted mantle plume component that interacted with enriched plume and (or) lithospheric mantle material shortly prior to eruption. The two sources identified for the Gardar rocks can be found with almost identical geochemical characteristics in the 1.14 Ga Abitibi dikes of the Superior Province, indicating a genetic link between the Gardar and the Abitibi magmas. The Aillik dikes of Labrador may represent a possible link between the two provinces, and contemporaneous metagabbros from the Grenville Province may also be related to this magmatic activity. The geochemical data lend support to the idea that the Gardar–Abitibi system was a major intracontinental rift zone similar to the present-day East African Rift. The recurrent activity for some 200 million years is consistent with models of a long-lived, pulsing superplume.

Acknowledgments

We thank M.M. Macouin and J.P. Valet for providing the Abitibi samples, G. Graser for help with sample preparation,

Fig. 10. Distribution of Eriksfjord Formation basalts and Isortoq and Abitibi dikes on (*a*) Hf/Ta vs. Ta/Th and (*b*) Ta/Yb vs. Hf/Yb diagrams. Similar diagrams were used by Condie (2005) to show mantle compositional components. Compositional fields for the high-U/Pb mantle (HIMU), enriched mantle (EM)1, and EM2 mantle components were taken from localities thought to reflect the respective end-member geochemical characteristics (Weaver 1991). Data sources: HIMU: Austral-Cook Islands (Chauvel et al. 1992, 1997; Hauri and Hart 1997); EM1: Kerguelen (Weis et al. 1998; Yang et al. 1998; Frey et al. 2000); EM2: Samoa (Workman et al. 2004). Compositions of primitive mantle (PM), depleted mid-ocean ridge basalt mantle (DMM), and normal mid-ocean ridge basalt (N-MORB) are from McDonough and Sun (1995), Workman and Hart (2005) and Sun and McDonough (1989), respectively. □, samples from Group 1; ●, samples from Group 2; inverted triangles, metagabbros from the Grenville Province (R.E. Ernst, unpublished data, on samples from A. Davidson).

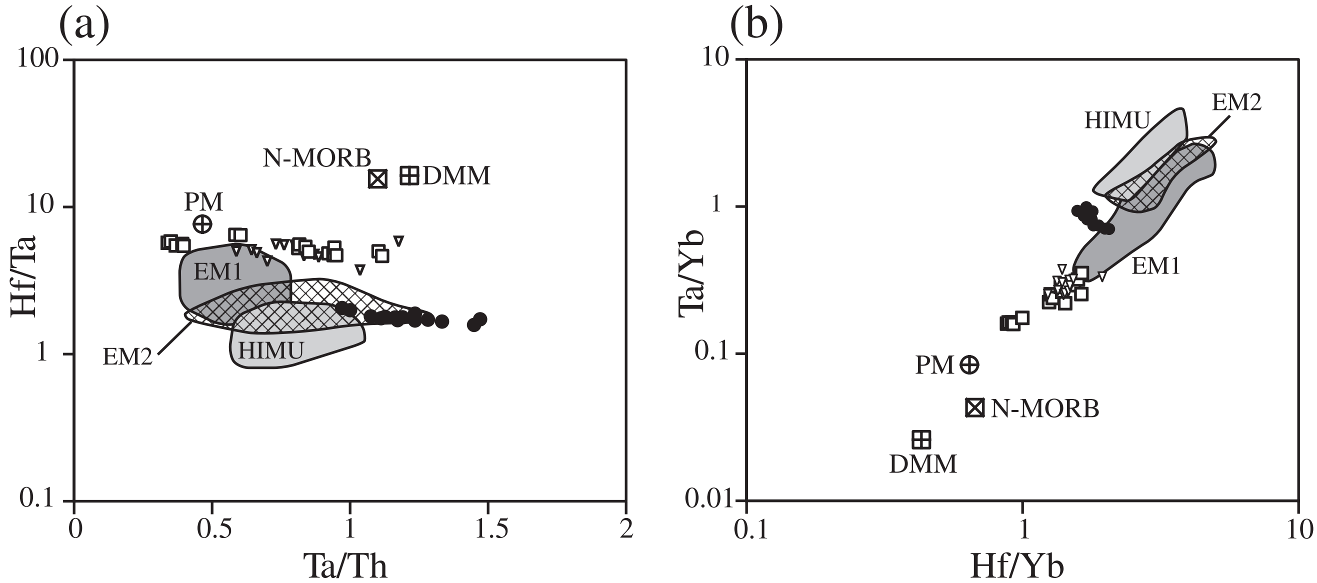

and J. Cotten for help with major element analysis. Constructive reviews by R. Ernst and an anonymous referee helped to improve the manuscript. J. Greenough is thanked for editing. R. Ernst provided access to his unpublished geochemical data on Canadian mafic rocks, which is greatly appreciated. Financial support from the European Volcano Dynamics Research Training Network is gratefully acknowledged.

References

Anderson, D.L. 2000. The thermal state of the upper mantle: no role for mantle plumes. Geophysical Research Letters, **27**: 3623–3626.

Anderson, D.L. 2005. Scoring hotspots: the plume and plate paradigms. *In* Plates, plumes, and paradigms. *Edited by* G.R. Foulger, J. Natland, D.C. Presnall, and D.L. Anderson. Geological Society of America, Special Paper 388, pp. 31–54.

Barrat, J.-A., Jahn, B.M., Joron, J.-L., Auvray, B., and Hamdi, H. 1990. Mantle heterogeneity in northeastern Africa: evidence from Nd isotopic compositions and hygromagmaphile element geochemistry of basaltic rocks from the Gulf of Tadjoura and southern Red Sea regions. Earth and Planetary Science Letters, **101**: 233–247.

Bell, K., and Simonetti, A. 1996. Carbonatite magmatism and plume activity: implications from the Nd, Pb and Sr isotope systematics of Oldoinyo Lengai. Journal of Petrology, **37**: 1321–1339.

Bell, K., and Tilton, G.R. 2001. Nd, Pb and Sr isotopic compositions of East African Carbonatites: evidence for mantle mixing and plume inhomogeneity. Journal of Petrology, **42**: 1927–1945.

Bernstein, S., Kelemen, P.B., Tegner, C., Kurz, M.D., Blusztajn, J., and Brooks, C.K. 1998. Post-breakup basaltic magmatism along the East Greenland Tertiary rifted margin. Earth and Planetary Science Letters, **160**: 845–862.

Bindeman, I.N., Davis, A.M., and Drake, M.J. 1998. Ion microprobe study of plagioclase-basalt partition experiments at natural concentration levels of trace elements. Geochimica et Cosmochimica Acta, **62**: 1175–1193.

Bonatti, E., Ottonello, G., and Hamlyn, P.R. 1986. Peridotites from the island of Zabargad (St. John), Red Sea: petrology and geochemistry. Journal of Geophysical Research, **91**(B1): 599–631.

Bridgwater, D. 1967. Feldspathic inclusions in the Gardar igneous rocks of South Greenland and their relevance to the formation of major anorthosites in the Canadian Shield. Canadian Journal of Earth Sciences, **4**: 995–1014.

Buchan, K.L., and Ernst, R.E. 2004. Diabase dyke swarms and related units in Canada and adjacent regions. Geological Survey of Canada, Map 2022A, scale 1 : 5 000 000.

Buchan, K.L., Hodych, J.P., Roddick, J.C., Emslie, R.F., and Hamilton, M.A. 1996. Paleomagnetism and U-Pb geochronology of Mesoproterozoic dykes of Labrador and correlations with dykes of southwest Greenland. *In* Proterozoic Evolution in the North Atlantic Realm. International Conference IGCP Project 371. *Compiled by* C.F. Gower. COPENA–ECSOOT–IBTA conference, Goose Bay, Labrador, 1996. Program and Abstracts, p. 37.

Buchan, K.L., Ernst, R.E., Hamilton, M.A., Mertanen, S., and Pesonen, L.J. 2001. Rodinia: the evidence from integrated paleomagnetism and U–Pb geochronology. Precambrian Research, **110**: 9–32.

Cadman, A.C., Heaman, L.M., Tarney, J., Wardle, R., and Krogh, T.E. 1993. U–Pb geochronology and geochemical variation within two Proterozoic mafic dyke swarms, Labrador. Canadian Journal of Earth Sciences, **30**: 1490–1504.

Cebriá, J.M., López-Ruiz, J., Doblas, M., Oyarzun, R., Hertogen, J., and Benito, R. 2000. Geochemistry of the Quaternary alkali basalts of Garrotxa (NE Volcanic Province, Spain): a case of double enrichment of the mantle lithosphere. Journal of Volcanology and Geothermal Research, **102**: 217–235.

Chauvel, C., Hofmann, A.W., and Vidal, P. 1992. HIMU–EM: the French–Polynesian connection. Earth and Planetary Science Letters, **110**: 99–119.

Chauvel, C., McDonough, W.F., Guille, G., Maury, R.C., and Duncan, R.A. 1997. Contrasting old and young volcanism in Rurutu Island, Austral Chain. Chemical Geology, **139**: 125–143.

Coffin, M.F., and Eldholm, O. 1994. Large igneous provinces: crustal structure, dimensions, and external consequences. Reviews of Geophysics, **32**: 1–36.

Condie, K.C. 2001. Mantle plumes and their record in Earth history. Cambridge University Press, Cambridge, UK.

Condie, K.C. 2003. Incompatible element ratios in oceanic basalts and komatiites: tracking deep mantle sources and continental growth rates with time. Geochemistry Geophysics Geosystems, **4**(1): 1005, doi:10.1029/2002GC000333.

Condie, K.C. 2005. High field strength element ratios in Archean basalts: a window to evolving sources of mantle plumes. Lithos, **79**: 491–504.

Condie, K.C., Bobrow, D.J., and Card, K.D. 1987. Geochemistry of Precambrian mafic dykes from the Southern Superior Province of the Canadian Shield. *In* Mafic dyke swarms. *Edited by* H.C. Halls and W.F. Fahrig. Geological Association of Canada, Special Paper 34, pp. 95–108.

Cook, C., Briggs, R.M., Smith, I.E.M., and Maas, R. 2005. Petrology and geochemistry of intraplate basalts in the South Auckland volcanic field, New Zealand: evidence for two coeval magma suites from distinct sources. Journal of Petrology, **46**: 473–503.

Cotten, J., Le Dez, A., Bau, M., Caroff, M., Maury, R.C., Dulski, P. et al. 1995. Origin of anomalous rare-earth element and yttrium enrichments in subaerially exposed basalts: evidence from French Polynesia. Chemical Geology, **119**: 115–138.

Coulson, I.M., Goodenough, K.M., Pearce, N.J.G., and Leng, M.J. 2003. Carbonatites and lamprophyres of the Gardar Province — a “window” to the sub-Gardar mantle? Mineralogical Magazine, **67**: 855–872.

Courtillot, V., Jaupart, C., Manighetti, I., Tapponnier, P., and Besse, J. 1999. On causal links between flood basalts and continental breakup. Earth and Planetary Science Letters, **166**: 177–195.

Davidson, A., and van Breemen, O. 1988. Baddeleyite-zircon relationships in coronitic metagabbro, Grenville Province, Ontario: implications for geochronology. Contributions to Mineralogy and Petrology, **100**: 291–299.

Davies, G.F. 1999. Dynamic Earth: plates, plumes and mantle convection. Cambridge University Press, Cambridge, UK.

Davis, D.W., and Paces, J.R. 1990. Time resolution of geologic events on the Keweenaw Peninsula and implications for development of the Midcontinent rift system. Earth and Planetary Science Letters, **97**: 54–64.

Eisele, J., Sharma, M., Galer, S.J.G., Blichert-Toft, J., Devey, C.W., and Hofmann, A.W. 2002. The role of sediment recycling in EM-1 inferred from Os, Pb, Hf, Nd, Sr isotope and trace element systematics of the Pitcairn hotspot. Earth and Planetary Science Letters, **196**: 197–212.

Ellam, R.M. 1992. Lithospheric thickness as a control on basalt geochemistry. Geology, **20**: 153–156.

Engell, J., and Pedersen, S. 1974: Rb–Sr whole rock isochron age determination from the Bangs Havn intrusion, South Greenland. Bulletin of the Geological Society of Denmark, **23**: 130–133.

Ernst, R.E., and Bell, K. 1992. Petrology of the Great Abitibi Dyke, Superior Province, Canada. Journal of Petrology, **33**: 423–469.

Ernst, R.E., and Buchan, K.L. 1993. Paleomagnetism of the Abitibi dyke swarm, southern Superior Province, and implications for the Logan Loop. Canadian Journal of Earth Sciences, **30**: 1886–1897.

Ernst, R.E., and Buchan, K.L. 1997. Giant radiating dyke swarms: their use in identifying pre-Mesozoic large igneous provinces and mantle plumes. *In* Large igneous provinces: continental, oceanic, and planetary flood volcanism. *Edited by* J.J. Mahoney and M.F. Coffin. American Geophysical Union, Geophysical Monograph 100, pp. 297–333.

Ernst, R.E., and Buchan, K.L. (*Editors*). 2001. Large mafic magmatic events through time and links to mantle-plume heads. *In* Mantle plumes: their identification through time. Geological Society of America, Special Paper 352, pp. 483–575.

Ernst, R.E., and Buchan, K.L. 2002. Maximum size and distribution in time and space of mantle plumes: evidence from large igneous provinces. Journal of Geodynamics, **34**: 309–342.

Ernst, R.E., and Hattori, K. 1992. Sr- and Nd-isotope study of mineral separates from the Great Abitibi Dyke, Canada. *In* International Geological Congress, Kyoto, Japan. Vol. 2, p. 567.

Fahrig, W.F. 1987. The tectonic settings of continental mafic dyke swarms: failed arm and early passive margin. *In* Mafic dyke swarms. *Edited by* H.C. Halls and W.F. Fahrig. Geological Association of Canada, Special Paper 34, pp. 331–348.

Fahrig, W.F., and Larochelle, A. 1972. Paleomagnetism of the Michael Gabbro and possible evidence of the rotation of Makkovik subprovince. Canadian Journal of Earth Sciences, **9**: 1287- 1296.

Finch, A.A., Mansfeld, J., and Andersen, T. 2001. U–Pb radiometric age of Nunarsuit pegmatite, Greenland: constraints of the timing of Gardar magmatism. Bulletin of the Geological Society of Denmark, **48**: 1–7.

Fitton, J.G., and James, D. 1986. Basic volcanism associated with intraplate linear features. Philosophical Transactions of the Royal Society of London, **A317:** 253–266.

Foulger, G.R., Natland, J.H., Presnall, D.C., and Anderson, D.L. (*Editors*). 2005. Plates, plumes, and paradigms. Geological Society of America, Special Paper 388.

Franz, G., Steiner, G., Volker, F., Pudlo, D., and Hammerschmidt, K. 1999. Plume related alkaline magmatism in central Africa — the Meidob Hills (W Sudan). Chemical Geology, **157**: 27–47.

Frey, F.A., Weis, D., Yang, H.-J., Nicolaysen, K., Leyrit, H., and Giret, A. 2000. Temporal geochemical trends in Kerguelen Archipelago basalts: evidence for decreasing magma supply from the Kerguelen plume. Chemical Geology, **164**: 61–80.

Garde, A.A., Hamilton, M.A., Chadwick, B., Grocott, J., and McCaffrey, K.J.W. 2002. The Ketilidian orogen of South Greenland: geochronology, tectonics, magmatism, and fore-arc accretion during Palaeoproterozoic oblique convergence. Canadian Journal of Earth Sciences, **39**: 765–793.

George, R.M., and Rogers, N.W. 2002. Plume dynamics beneath the African plate inferred from the geochemistry of the Tertiary basalts of southern Ethiopia. Contributions to Mineralogy and Petrology, **144**: 286–304.

Gibson, I.L., Sinha, M.N., and Fahrig, W.F. 1987. The geochemistry of the Mackenzie dyke swarm, Canada. *In* Mafic dyke swarms. *Edited by* H.C. Halls and W.F. Fahrig. Geological Association of Canada, Special Paper 34, pp. 109–121.

Goodenough, K.M., Upton, B.G.J., and Ellam, R.M. 2002. Long-term memory of subduction processes in the lithospheric mantle: evidence from the geochemistry of basic dykes in the Gardar Province of south Greenland. Journal of the Geological Society (of London), **159**: 705–714.

Green, D.H., and Ringwood, A.E. 1967. The stability fields of aluminous pyroxene peridotite and garnet peridotite and their relevance in upper mantle structure. Earth and Planetary Science Letters, **3**: 151–160.

Haase, K.M., Goldschmidt, B., and Garbe-Schönberg, C.D. 2004. Petrogenesis of Tertiary continental intra-plate lavas from the Westerwald region, Germany. Journal of Petrology, **45**: 883–905.

Halama, R., Waight, T., and Markl, G. 2002. Geochemical and isotopic zoning patterns of plagioclase megacrysts in gabbroic dykes from the Gardar Province, South Greenland: implications for crystallisation processes in anorthositic magmas. Contributions to Mineralogy and Petrology, **144**: 109–127.

Halama, R., Wenzel, T., Upton, B.G.J., Siebel, W., and Markl, G. 2003. A geochemical and Sr-Nd-O isotopic study of the Proterozoic Eriksfjord basalts, Gardar Province, South Greenland: reconstruction of an OIB signature in crustally contaminated rift-related basalts. Mineralogical Magazine, **67**: 831–853.

Halama, R., Marks, M., Brügmann, G., Siebel, W., Wenzel, T., and Markl, G. 2004. Crustal contamination of mafic magmas: evidence from a petrological, geochemical and Sr–Nd–Os–O isotopic study of the Proterozoic Isortoq dike swarm, South Greenland. Lithos, **74**: 199–232.

Halliday, A.N., Lee, D.-C., Tommasini, S., Davies, G.R., Paslick, C.R., Fitton, J.G. et al. 1995. Incompatible trace elements in OIB and MORB and source enrichment in the sub-oceanic mantle. Earth and Planetary Science Letters, **133**: 379–395.

Hart, S.R., Hauri, E.H., Oschmann, L.A., and Whitehead, J.A. 1992. Mantle plumes and entrainment: isotopic evidence. Science, **256**: 517–520.

Hauri, E.H., and Hart, S.R. 1997. Rhenium abundances and systematics in oceanic basalts. Chemical Geology, **139**: 185–205.

Hawkesworth, C.J., Rogers, N.W., van Calsteren, P.W.C., and Menzies, M.A. 1984. Mantle enrichment processes. Nature, **311**: 331–335.

Hawkesworth, C.J., Mantovani, M.S.M., Taylor, P.N., and Palacz, Z. 1986. Evidence from the Parana of South Brazil for a continental contribution to Dupal basalts. Nature, **322**: 356–359.

Hoffman, P.F. 1989. Speculations on Laurentia's first gigayear (2.0 to 1.0 Ga). Geology, **17**: 135–138.

Hofmann, A.W. 1997. Mantle geochemistry: the message from oceanic volcanism. Nature, **385**: 219–229.

Hofmann, A.W. 2003. Sampling mantle heterogeneity through oceanic basalts: isotopes and trace elements. *In* The mantle and core. Treatise on geochemistry. *Edited by* R.W. Carlson. Vol. 2, pp. 61–101.

Hofmann, A.W., and White, W.M. 1982. Mantle plumes from ancient oceanic crust. Earth and Planetary Science Letters, **79**: 33–45.

Hofmann, A.W., and White, W.M. 1983. Ba, Rb, and Cs in the Earth's mantle. Zeitschrift für Naturforschung, **38**: 256–266.

Ito, G. 2001. Reykjanes 'V'-shaped ridges originating from a pulsing and dehydrating mantle plume. Nature, **411**: 681–684.

Johnson, J.S., Gibson, S.A., Thompson, R.N., and Nowell, G.M. 2005. Volcanism in the Vitim volcanic field, Siberia: geochemical evidence for a mantle plume beneath the Baikal rift zone. Journal of Petrology, **46**: 1309–1344.

Joron, J.-L. 2000. Eléments hygromagmaphiles : concepts, méthodes d'étude. Applications à l'étude de la pétrogénèse des magmas et aux propriétés de leurs sources mantelliques. Mise au point et valorisation d'un outil géochimique : l'analyse par activation. Doctorat d'Etat, Université Paris 7.

Joron, J.-L., and Treuil, M. 1989. Hygromagmaphile element distributions in oceanic basalts as fingerprints of partial melting and mantle heterogeneities: a specific approach and proposal of an identification and modelling method. *In* Magmatism in the ocean basins. *Edited by* A.D. Saunders and M.J. Norry. Geological Society (of London), Special Publication 42, pp. 277–299.

Joron, J.-L., Treuil, M., and Raimbault, L. 1997. Activation analysis as a geochemical tool: Statement of capabilities for geochemical trace element studies. Journal of Radioanalytical and Nuclear Chemistry, **216**: 229–235.

Kelemen, P.B., Dick, H.J.B., and Quick, J.E. 1992. Formation of harzburgite by pervasive melt/rock reaction in the upper mantle. Nature, **358**: 635–641.

Kelemen, P.B., Shimizu, N., and Dunn, T. 1993. Relative depletion of niobium in some arc magmas and the continental crust: partitioning of K, Nb, La and Ce during melt/rock reaction in the upper mantle. Earth and Planetary Science Letters, **120**: 111–134.

Kempton, P.D., Fitton, J.G., Saunders, A.D., Nowell, G.M., Taylor, R.N., Hardason, B.S. et al. 2000. The Iceland plume in space and time: a Sr–Nd–Pb–Hf study of the North Atlantic rifted margin. Earth and Planetary Science Letters, **177**: 255–271.

Kerr, A.C., Saunders, A.D., Tarney, J., Berry, N.H., and Hards, V.L. 1995. Depleted mantle-plume geochemical signatures: no paradox for plume theories. Geology, **23**: 843–846.

Krogh, T.E., Corfu, F., Davis, D.W., Dunning, G.R., Heaman, L.M., Kamo, S.L. et al. 1987. Precise U-Pb isotopic ages of diabase dykes and mafic to ultramafic rocks using trace amounts of baddeleyite and zircon. *In* Mafic dyke swarms. *Edited by* H.C. Halls and W.F. Fahrig. Geological Association of Canada, Special Paper 34, pp. 147–152.

Krumrei, T.V., Villa, I.M., Marks, A.W., and Markl, G. 2006. A ^{40}Ar/^{39}Ar and U/Pb isotopic study of the Ilimaussaq complex, South Greenland: Implications for the ^{40}K decay constant and for the duration of magmatic activity in a peralkaline complex. Chemical Geology, **227**: 258–273.

Larsen, J.G. 1977. Petrology of the late lavas of the Eriksfjord Formation, Gardar Province, South Greenland. Bulletin Grønlands Geologiske Undersøgelse, **125**: 1–31.

Lin, S.-C., and van Keken, P.E. 2005. Multiple volcanic episodes of flood basalts caused by thermochemical plumes. Nature, **436**: 250–252.

Macdonald, R., and Upton, B.G.J. 1993. The Proterozoic Gardar rift zone, south Greenland: comparisons with the East African Rift System. *In* Magmatic processes and plate tectonics. *Edited by* H.M. Pritchard, T. Alabaster, N.B.W. Harris, and C.R. Neary. Geological Society (of London), Special Publication 76, pp. 427–442.

Macouin, M., Valet, J.P., Besse, J., Buchan, K., Ernst, R., LeGoff, M. et al. 2003. Low paleointensities recorded in 1 to 2.4 Ga Proterozoic dykes, Superior Province, Canada. Earth and Planetary Science Letters, **213**: 79–95.

McDonough, W.F., and Sun, S.-S. 1995. The composition of the Earth. Chemical Geology, **120**: 223–253.

McHone, J.G., Anderson, D.L., Beutel, E.K., and Fialko, Y.A. 2005. Giant dikes, rifts, flood basalts, and plate tectonics: a contention of mantle models. *In* Plates, plumes, and paradigms. *Edited by* G.R. Foulger, J. Natland, D.C. Presnall, and D.L. Anderson. Geological Society of America, Special Paper 388, pp. 401–420.

McKenzie, D., and O'Nions, R.K. 1991. Partial melt distributions from inversion of rare earth element concentrations. Journal of Petrology, **32**: 1021–1091.

Morgan, W.J. 1971. Convection plumes in the lower mantle. Nature, **230**: 42–43.

Nelson, D.R., Chivas, A.R., Chappell, B.W., and McCulloch, M.T. 1988. Geochemical and isotopic systematics in carbonatites and implications for the evolution of ocean-island sources. Geochimica et Cosmochimica Acta, **52**: 1–17.

Nicholson, S.W., Shirey, S.B., Schulz, K.J., and Green, J.C. 1997. Rift-wide correlation of 1.1 Ga Midcontinent rift system basalts:

implications for multiple mantle sources during rift development. Canadian Journal of Earth Sciences, **34**: 504–520.

O'Connor, J.M., Stoffers, P., Wijbrans, J.R., Shannon, P.M., and Morrissey, T. 2000. Evidence from episodic seamount volcanism for pulsing of the Iceland plume in the past 70 Myr. Nature, **408**: 954–958.

Okamura, S., Arculus, R.J., and Martynov, Y.A. 2005. Cenozoic magmatism of the North-Eastern Eurasian margin: the role of lithosphere versus asthenosphere. Journal of Petrology, **46**: 221–253.

Paces, J.R., and Bell, K. 1989. Non-depleted sub-continental mantle beneath the Superior Province of the Canadian Shield: Nd–Sr isotopic and trace element evidence from Midcontinent Rift basalts. Geochimica et Cosmochimica Acta, **53**: 2023–2035.

Paslick, C.R., Halliday, A.N., Davies, G.R., Mezger, K., and Upton, B.G.J. 1993. Timing of Proterozoic magmatism in the Gardar Province, southern Greenland. Bulletin of the Geological Society of America, **105**: 272–278.

Pilet, S., Hernandez, J., Sylvester, P., and Poujol, M. 2005. The metasomatic alternative for ocean island basalt chemical heterogeneity. Earth and Planetary Science Letters, **236**: 148–166.

Piper, J.D.A., Thomas, D.N., Share, S., and Rui, Z.Q. 1999. The palaeomagnetism of (Mesoproterozoic) Eriksfjord Group red beds, South Greenland: multiphase remagnetization during the Gardar and Grenville episodes. Geophysical Journal International, **136**: 739–756.

Reichow, M.K., Saunders, A.D., White, R.V., Al'Mukhamedov, A.I., and Medvedev, A.Ya. 2005. Geochemistry and petrogenesis of basalts from the West Siberian Basin: an extension of the Permo-Triassic Siberian Traps, Russia. Lithos, **79**: 425–452.

Robinson, J.A.C., and Wood, B.J. 1998. The depth of the spinel to garnet transition at the peridotite solidus. Earth and Planetary Science Letters, **164**: 277–284.

Rollinson, H. 1993. Using geochemical data: evaluation, presentation, interpretation. Longman Group UK Limited, London, UK.

Salters, V.J.M., and Longhi, J. 1999. Trace element partitioning during the initial stages of melting beneath mid-ocean ridges. Earth and Planetary Science Letters, **166**: 15–30.

Salters, V.J.M., Longhi, J., and Bizimis, M. 2002. Near mantle solidus trace element partitioning at pressures up to 3.4 GPa. Geochemistry Geophysics Geosystems, **3**(7), doi 10.1029/2001GC000148.

Schilling, J.-G. 1973. Iceland mantle plume: geochemical evidence along Reykjanes Ridge. Nature, **242**: 565–571.

Shaw, D.M. 1970. Trace element fractionation during anatexis. Geochimica et Cosmochimica Acta, **34**: 237–243.

Sleep, N.H. 1997. Lateral flow and ponding of starting plume material. Journal of Geophysical Research, **102**(B5): 10 001 – 10 012.

Smith, A.D. 2005. The streaky-mantle alternative to mantle plumes and its bearing on bulk-Earth geochemical evolution. *In* Plates, plumes, and paradigms. *Edited by* G.R. Foulger, J. Natland, D.C. Presnall, and D.L. Anderson. Geological Society of America, Special Paper 388, pp. 303–325.

Sun, S.-S., and McDonough, W.F. 1989. Chemical and isotopic systematics of oceanic basalts: implications for mantle composition and processes. *In* Magmatism in the ocean basins. *Edited by* A.D. Saunders and M.J. Norry. Geological Society (of London), Special Publication 42, pp. 313–345.

Tarney, J., and Weaver, B.L. 1987. Geochemistry and petrogenesis of Early Proterozoic dyke swarms. *In* Mafic dyke swarms. *Edited by* H.C. Halls and W.F. Fahrig. Geological Association of Canada, Special Paper 34, pp. 81–94.

Thompson, R.N., and Gibson, S.A. 1991. Subcontinental mantle plumes, hotspots and pre-existing thinspots. Journal of the Geological Society (of London), **148**: 973–977.

Upton, B.G.J. 1991. Gardar mantle xenoliths: Igdlutalik, South Greenland. Rapport – Grønlands Geologiske Undersoegelse, **150**: 37–43.

Upton, B.G.J., and Emeleus, C.H. 1987. Mid-Proterozoic alkaline magmatism in southern Greenland: the Gardar Province. *In* Alkaline igneous rocks. *Edited by* J.G. Fitton and B.G.J. Upton. Geological Society (of London), Special Publication 30, pp. 449–471.

Upton, B.G.J., Emeleus, C.H., Heaman, L.M., Goodenough, K.M., and Finch, A.A. 2003. Magmatism of the mid-Proterozoic Gardar Province, South Greenland: chronology, petrogenesis and geological setting. Lithos, **68**: 43–65.

Van Keken, P.E., Ballentine, C.J., and Hauri, E.H. 2003. Convective mixing in the Earth's mantle. *In* The mantle and core. Treatise on Geochemistry. *Edited by* R.W. Carlson. Vol. 2, pp. 471–491.

Weaver, B.L. 1991. Trace element evidence for the origin of ocean-island basalts. Geology, **19**: 123–126.

Weaver, B.L., Wood, D.A., Tarney, J., and Joron, J.-L. 1986. Role of subducted sediment in the genesis of ocean-island basalts: geochemical evidence from South Atlantic Ocean islands. Geology, **14**: 275–278.

Weis, D., Frey, F.A., Giret, A., and Cantagrel, J.-M. 1998. Geochemical characteristics of the youngest volcano (Mount Ross) in the Kerguelen Archipelago: inferences for magma flux, lithosphere assimilation and composition of the Kerguelen plume. Journal of Petrology, **39**: 973–994.

Wilband, J.T., and Wasuwanich, P. 1980. Models of basalt petrogenesis: Lower Keweenawan diabase dikes and Middle Keweenawan Portage Lake lavas, Upper Michigan. Contributions to Mineralogy and Petrology, **75**: 395–406.

Workman, R.K., and Hart, S.R. 2005. Major and trace element composition of the depleted MORB mantle (DMM). Earth and Planetary Science Letters, **231**: 53–72.

Workman, R.K., Hart, S.R., Jackson, M., Regelous, M., Farley, K.A., Blusztajn, J., Kurz, M., and Staudigel, H. 2004. Recycled metasomatized lithosphere as the origin of the Enriched Mantle II (EM2) end-member: evidence from the Samoan volcanic chain. Geochemistry Geophysics Geosystems, **5:** Q04008, doi:10.1029/2003GC000623.

Yang, H.-J., Frey, F.A., Weis, D., Giret, A., Pyle, D., and Michon G. 1998. Petrogenesis of the flood basalts forming the Northern Kerguelen Archipelago: implications for the Kerguelen plume. Journal of Petrology, **39**: 711–748.

Yarmoluk, V.V., Kovalenko, V.I., and Kzmin, M.I. 2000. North Asia superplume activity in the Phanerozoic: magmatism and geodynamics. Geotectonics, **34**: 343–366.

Appendix A

Geographic coordinates of Abitibi samples (from Macouin et al. 2003):

Q2: 48°22′50.9″N, 77°58′32.7″W
Q7: 48°53′19.7″N, 79°30′17.0″W
T1: 48°10′56.1″N, 81°34′58.7″W
T2: 48°10′56.2″N, 81°34′58.8″W
T3: 48°11′59.7″N, 80°34′00.1″W